VOLUME IV JANUARY, 1939 NUMBER 1

GEOPHYSICS

A Journal of General and Applied Geophysics

MAXIMUM ELECTROMAGNETIC DAMPING OF A RELUCTANCE SEISMOMETER*

NEIL R. SPARKS AND PAUL F. HAWLEY†

ABSTRACT

An explicit solution of the third order differential equation of motion of an electromagnetically damped reluctance seismometer is obtained for the case of greatest interest, i.e., when the terminating resistor is adjusted to give greatest damping. This solution shows that definite inter-relationships among the instrument constants are necessary for appreciable damping. The theoretical limitations on the maximum damping which can be obtained are discussed.

The mathematical treatment of the response of the oil damped seismometer so widely used in geophysical prospecting has been simple and complete. The theoretical results have been fairly well checked against experiments. As far as we know no such analysis has been published for the electromagnetically damped reluctance seismometer.

The difficulty in determining mathematically the response of an electromagnetically damped reluctance seismometer arises from the fact that the equation of motion is not a simple second order differential equation as is the case of the oil damped seismometer, but is a third order equation. Except in special cases, explicit solutions of such equations cannot be obtained.

We have succeeded in obtaining an explicit solution of the equation of motion for the case of maximum damping, and as a consequence, the relations which must hold among the seismometer constants—mass, spring, damping resistor, etc. for this special case.

When a unit force is applied to the sprung mass of a balanced armature reluctance seismometer, the differential equation of the

* Paper read at Annual Meeting, New Orleans, La., March 16, 1938.

† Geophysical Laboratory, Stanolind Oil and Gas Company; Tulsa, Okla.

voltage across the terminating resistor in terms of the seismometer constants is:

$$\frac{d^3e}{dt^3}+\frac{R}{L}\cdot\frac{d^2e}{dt}+\left(\frac{S-S''}{M}+\frac{S''}{M}\cdot\frac{L-L''}{L}\right)\frac{de}{dt}+\frac{S-S''}{M}\cdot\frac{R}{L}\cdot e=0. \qquad (1)$$

The derivation of equation (1) can be obtained from Washburn's work.[1]

In this equation e is the output voltage across the damping resistor R, L is the total seismometer inductance, L'' is the leakage inductance, S is the spring constant, S'' the negative equivalent spring constant due to the unbalanced magnetic pull on the armature, and M is the sprung mass.

Equation (1) can be simplified by expressing the coefficients of the various terms by single letters:

$$\frac{S-S''}{M}=\omega_0^2,\quad \frac{R}{L}=D \quad \text{and} \quad \left(\frac{S-S''}{M}+\frac{S''}{M}\cdot\frac{L-L''}{L}\right)=\omega_1^2.$$

This gives:

$$\frac{d^3e}{dt^3}+D\cdot\frac{d^2e}{dt^2}+\omega_1^2\cdot\frac{de}{dt}+D\cdot\omega_0^2\cdot e=0. \qquad (2)$$

The significance of the choice of symbols can best be seen from equation (2) for certain values of terminating resistance.

Case A: $R=\infty\,(D=\infty)$ (open circuit).

Equation (2) becomes

$$\frac{d^2e}{dt^2}+\omega_0^2e=0. \qquad (2a)$$

Therefore $\omega_0=2\pi f_0$ where $f_0=$ the natural frequency of oscillation on open circuit.

Case B: $R=0\,(D=0)$ (short circuit);

$$\frac{d^3e}{dt^3}+\omega_1^2\frac{de}{dt}=0. \qquad (2b)$$

Therefore $\omega_1=2\pi f_1$ where $f_1=$ the natural frequency of oscillation on short circuit.

[1] Experimental Determination of the Transient Characteristics of Seismographic Apparatus. Harold W. Washburn, GEOPHYSICS, Volume II, Number 3, July 1937.

The general solution of equation (2), as for any other linear differential equation with constant coefficients, has the form $e=E\cdot\epsilon^{mt}$ where m is real or complex. If we substitute this general expression into the differential equation, we obtain an equation in m which is

$$m^3 + Dm^2 + \omega_1^2 m + D\omega_0^2 = 0. \tag{3}$$

There are three values of m which satisfy equation (3), at least one of which must be real. Since in general, the output of the seismometer is oscillatory, the two other values of m are complex and conjugate.

Consider either of the roots that make up the oscillatory part of the solution. m, being complex, has the form $\alpha+j\beta$ where α is the damping constant and β the damped angular frequency.

The substitution of $\alpha+j\beta$ for m gives rise to a complex equation in which the real and imaginary parts must vanish independently. Thus, there are two equations involving α, β, and the constants of the seismometer.

$$\alpha^3 + 3\alpha\beta^2 + D\alpha^2 - D\beta^2 + \omega_1^2\alpha + D\omega_0^2 = 0 \tag{4}$$

$$\beta(3\alpha^2 - \beta^2 + 2D\alpha + \omega_1^2) = 0 \tag{5}$$

β can be eliminated, yielding one equation in α and the seismometer constants:

$$8\alpha^3 + 8D\alpha^2 + 2(\omega_1^2 + D^2)\alpha + D(\omega_1^2 - \omega_0^2) = 0. \tag{6}$$

The derivation of a general explicit solution of equation (6) for α is hopeless. Even a numerical solution gives the damping constant for only one particular set of values of the seismometer constants.

It is evident from the substitution of numerical values and more particularly from tests on actual seismometers that for any given set of seismometer constants $-S$, S'', M, L and L'' there is a certain value of terminating resistance which gives maximum damping. Therefore, we investigated this equation to see if an explicit solution for this particular value of resistance could be obtained in terms of the other seismometer constants. To do this we allowed the only term containing R, i.e., D, to vary, then maximized by the usual process of setting $(d\alpha/dD)=0$ in the above equation.

$$\frac{d\alpha}{dD} = -\frac{8\alpha^2 + 4D\alpha + \omega_1^2 - \omega_0^2}{24\alpha^2 + 16D\alpha + 2(\omega_1^2 + D^2)}. \tag{7}$$

Therefore

$$8\alpha_m^2 + 4D_m\cdot\alpha_m + \omega_1^2 - \omega_0^2 = 0, \tag{8}$$

where α_m and D_m are values of α and D which give maximum damping. This is the key to the explicit solution. The value of α resulting from this process is a single-valued explicit function of ω_1 and ω_0. Solving equations (6) and (8) simultaneously, we get

$$\frac{\alpha_m}{\omega_0} = -\frac{\omega_1^2 - \omega_0^2}{4\omega_0^2} \tag{9}$$

or from the original definitions

$$\frac{\alpha_m}{\omega_0} = -\frac{S''/S}{1 - S''/S}\cdot\frac{L - L''}{4L} \tag{9a}$$

and

$$D_m = \frac{\omega_1^2 + \omega_0^2}{2\omega_0} = \frac{R_m}{L}\,. \tag{10}$$

The substitution of equations (9) and (10) in equation (5) gives

$$\beta_m = \omega_0\left[1 + \frac{\omega_1^2 - \omega_0^2}{2\omega_0^2} - \left(\frac{\omega_1^2 - \omega_0^2}{4\omega_0^2}\right)^2\right]^{1/2} \tag{11}$$

or, the frequency of the damped oscillation is

$$f_m = f_0\left[1 + \frac{\omega_1^2 - \omega_0^2}{2\omega_0^2} - \left(\frac{\omega_1^2 - \omega_0^2}{4\omega_0^2}\right)^2\right]^{1/2} \tag{12}$$

where $f_0 = \frac{\omega_0}{2\pi}$ is the "open circuit" frequency of the seismometer.

The third root of the equation is obtained by dividing equation (3) by the product of the two known roots $(m-\alpha-j\beta)(m-\alpha+j\beta)$, giving

$$m_3 = -\omega_0. \tag{13}$$

Knowing the values for the three roots as given above, the complete explicit solution of the original differential equation for the special case of maximum electromagnetic damping, which is less than critical, can be expressed as the sum of a damped oscillation and a non-oscillatory term,

$$e = E_1\cdot\epsilon^{\alpha t}\cdot\sin(\beta t - \delta) + E_2\epsilon^{-\omega_0 t} \tag{14}$$

where E_1, E_2 and δ depend on the initial conditions.

When a small weight is removed from the sprung mass of the seismometer, the response expressed in the form of equation (14) becomes

$$e = E \cdot \epsilon^{\alpha t} \cdot \sin(\beta t - \delta) + E \cdot \frac{\beta}{\omega_0 \sqrt{2}} \cdot \epsilon^{-\omega_0 t} \qquad (15)$$

where

$$\sin \delta = \frac{\beta}{\omega_0 \sqrt{2}} .$$

It is interesting to examine the form of this equation. The oscillatory term has the same form as that of an oil damped seismometer

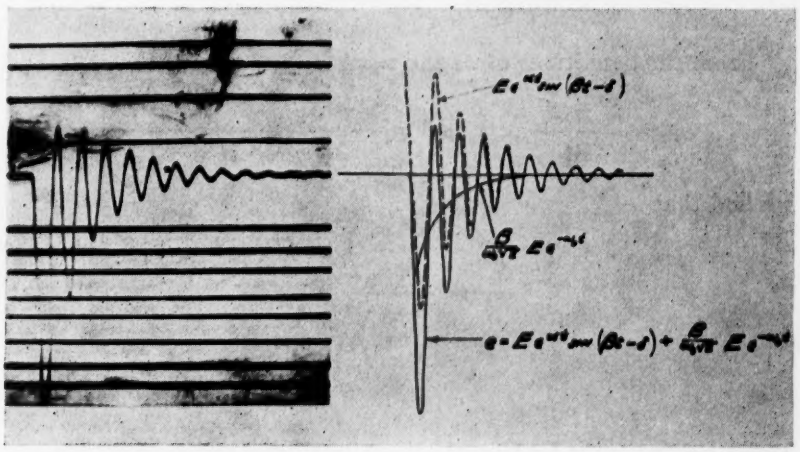

FIG. 1. Observed and theoretical response of an electromagnetically damped balanced armature type reluctance seismometer to a unit function force.

after a unit force is applied. Superimposed on this is an exponential term which in effect shifts the zero axis of the oscillatory term. That this solution gives the correct qualitative picture of the electromagnetically damped seismometer response is evident from the comparison of the forms of the theoretical curve and the test oscillogram shown in Fig. 1.

It should be particularly noted that the maximum damping referred to so far in this work is solely the maximum attainable with fixed values of S, S'', M, L, and L'' and is not necessarily the ultimate value for this type of seismometer. As can be readily seen from equation (9a), the damping depends on the ratio S''/S and is theoretically unlimited as S''/S approaches 1. However, as S''/S approaches

1, the seismometer becomes unstable, i.e., the armature tends to stick to the pole faces. Therefore, the ultimate value electromagnetic damping which can be obtained in a practical seismometer of this type is determined by the stability required.

Critical damping is the ultimate value of damping that is ordinarily desired. The definition of critical damping as that value of damping at which the output is non-oscillatory following the application of unit force, requires that $\beta \equiv 0$.

Solving equation (11) for $\beta = 0$ gives

$$\frac{\omega_1}{\omega_0} = \sqrt{5 + 4\sqrt{2}} = \sqrt{10.656} = 3.26. \tag{16}$$

From the definitions of ω_0 and ω_1

$$\omega_0^2 = \frac{S - S''}{M}, \qquad \omega_1^2 = \frac{S - S''}{M} + \frac{S''}{M} \cdot \frac{L - L''}{L},$$

we find that

$$\frac{S''}{S} = \frac{\left(\frac{\omega_1}{\omega_0}\right)^2 - 1}{\left(\frac{\omega_1}{\omega_0}\right)^2 - \frac{L''}{L}}. \tag{17}$$

Since $0 < \frac{L''}{L} < 1$,

$$\frac{\left(\frac{\omega_1}{\omega_0}\right)^2 - 1}{\left(\frac{\omega_1}{\omega_0}\right)^2} < \frac{S''}{S} < 1.$$

From equation (17) for $L''/L = 0$ and critical damping

$$\frac{S''}{S} = \frac{10.656 - 1}{10.656} = 0.905.$$

Therefore, $0.905 < S''/S < 1$, i.e., S'' (negative equivalent spring constant due to unbalanced magnetic pull of the armature) must be greater than 90% of S (spring constant) before the reluctance seismometer can be "critically" damped (electromagnetically).

A point which should be stressed is that this work applies strictly only to an ideal seismometer. The assumptions which have been made to obtain the original equation have been enumerated by Washburn.[2] The differences between this theoretical instrument and an actual seismometer have been discussed by Silverman.[3] Due to these differences, the results obtained in this paper are to be considered as providing a qualitative guide to performance rather than a complete quantitative prediction of results.

[2] Loc. cit.

[3] The Frequency Response of Electromagnetically Damped Dynamic and Reluctance Type Seismometers. Daniel Silverman, GEOPHYSICS, this number.

ON SEISMIC PATHS AND VELOCITY-TIME RELATIONS*

M. MOTT-SMITH†

ABSTRACT

It is shown that only a few very simple velocity-depth laws lead to path equations that can be integrated, and that none of them are suitable for application, either because there are no empirical velocities to which they conform sufficiently closely, or because the difficulties of fitting them to an empirical velocity are too great. It is shown that there are velocity-time relations that do conform closely to the usual form of an empirical velocity, relations which can be easily fitted to the latter, which are not difficult to handle, and which have other advantages. Two ways of applying the seismic paths are discussed.

Seismic computations are based for the most part on the assumption that the seismic paths are straight. The variation of the velocity with the depth, as determined by observations, is allowed for, but the curvature of the path produced by that variation is ignored. There is a certain inconsistency in this. But it is more or less of a compulsory inconsistency. The difficulties and complications of taking account of the curvature are so great that they are naturally shunned. Furthermore, it is felt that in deep reflection shooting, the rays being nearly vertical, the curvature is slight and may safely be ignored. This belief is confirmed by such curvature investigations as have been made. So long as the reflecting beds are deep and not far from horizontal the curvature errors are small and do not in general exceed the observation errors. But when the beds are shallow or the dips are steep or the velocity varies rapidly with the depth, the curvature errors become large and should be taken into account.

The practical determination of these errors, however, is beset with very great mathematical difficulties. One must substitute for the empirically determined velocity a mathematical curve corresponding to some equation, and the paths and the dips and depths derived from this equation apply of course to the substituted curve. They apply to the empirical curve only in so far as the former fits the latter. If the fit is poor, the errors of misfit may exceed those of curvature, so that the results are worse than if no corrections had been attempted. It is important therefore that the mathematical curve be of such a nature that it can be fitted closely to the empirical one; and it is desirable that it also be of such a nature that least squares can be applied for this purpose.

* Paper received Nov. 21, 1938.

† Independent Exploration Company, Houston, Texas.

One could avoid the use of a mathematical curve by dividing the underground region into a number of layers and determining an average velocity for each layer from the given empirical velocity. By calculating the refraction angle at each interface he could then trace the course of a ray as a broken line. He would at least be sure that this ray followed the actually observed velocity rather than a poor imitation of it. But this is a long and highly inaccurate process, since the errors are cumulative. Unless a great number of layers is used, the broken line represents the real path very inadequately; and if a great number of layers is used, the error accumulated at the end becomes enormous. The process has to be repeated for every ray, and when at last a whole chart of ray paths and wave fronts has been produced, that is only the beginning of one's troubles. The real difficulties arise when the attempt is made to apply the paths or their equations to the determination of dips and depths, or of corrections for them when calculated on the straight line assumption. The only exception is a vertical shot with a short spread. In this case, with the aid of an approximation, the desired quantities can be found quite simply.

For a complete and satisfactory solution, therefore, the use of a mathematical equation cannot be avoided. There is no especial difficulty in finding an equation to fit almost any empirical curve that is not too irregular. But here another requirement steps in. The equation, or more exactly that of the corresponding instantaneous velocity, must be such that the differential path equations to which it leads can be integrated. There are only a few simple relations that meet this requirement. Of course, any expression can be integrated by expanding it into a series. But most of these series are strongly convergent only for small angles, whereas it is precisely the large angles or steep dips that require correction. If a large number of terms running up to high powers is required for sufficient accuracy, it becomes almost impossible to solve the equation for the angle. The process of computing the corrections is at best extremely long and complicated. Hence it is desirable that the equations when integrated shall still be quite simple.

For these reasons, those who have investigated seismic paths theoretically have assumed very simple velocity-depth laws. These are of three types.

I. The parabolic type without initial velocity, whose general equation is:

$$V = Az^{1/n}$$

where $n \geqq 1$, and A is the slope constant. The velocity then varies as some root of the depth. A and n are adjusted so as fit the given empirical velocity as closely as this particular equation permits.

II. The parabolic type with initial velocity, whose general equation is:

$$V = V_0 + Az^{1/n}$$

where V_0 is the initial velocity.

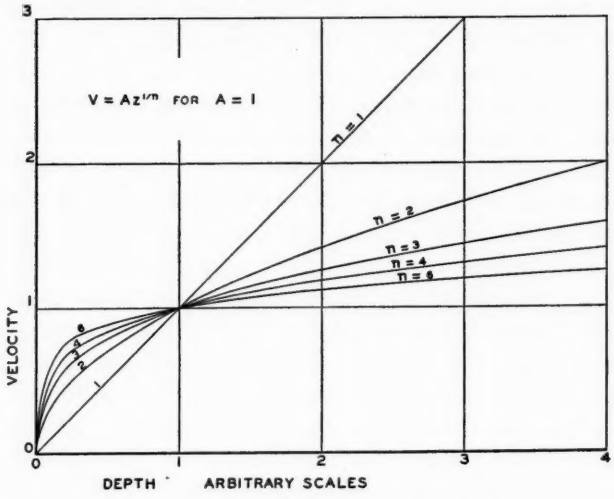

FIG. 1.

III. The exponential type, whose equation is:

$$V = V_0 e^{Az}.$$

I. The forms of the parabolic family without initial velocity are shown in Fig. 1. The scales are arbitrary and $A = 1$, since the purpose is merely to show the forms. All the curves start the positive part at the origin. When $n = 1$, the curve is a straight line. When $n = 2$, the curve is the ordinary parabola. When $n > 1$, the curves rise more sharply at first, but are flatter in the end. Each parabola has its vertex at the origin, and the Z axis as its axis.

All of these parabolas lead to differential path equations that can be integrated by elementary means if n is an integer, or with the help of Gamma functions if n is not an integer.

But these parabolas, being instantaneous velocity curves, are not the ones to be fitted to a given empirical velocity. Before the fitting

can be started, the corresponding average velocity curves must be derived.

One could of course do the reverse, consider these parabolas as average velocity curves, fit one to the empirical velocity, derive the corresponding instantaneous velocity, and from the latter the path equations. It happens in this case that, except for $n=1$, both sets of

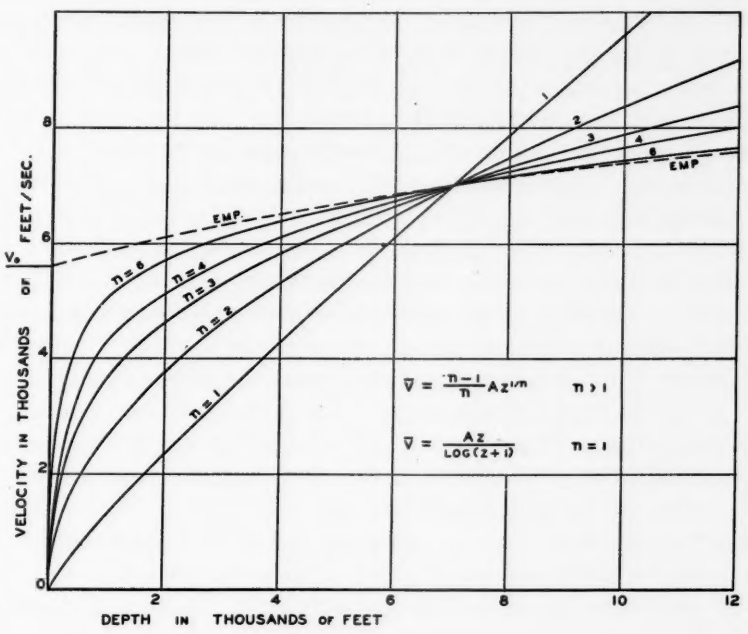

FIG. 2.

equations are of the same form and equally simple. But in general the derived equation, whether it be the average or the instantaneous one, is the more complicated. Since it is necessary that the equation from which the seismic paths are to be derived be as simple as possible, it is better to fit the derived equation to the empirical velocity.

Fig. 2 shows the average velocity curves corresponding to the parabolas of Fig. 1. From the equations of these curves given on the figure, it will be noted that, except for $n=1$, they differ from those for the parabolas of Fig. 1 only in the value of the constant coefficient. They are hence of the same form, namely, parabolas, with their vertices at the origin, and the Z axis as their axis. For $n=1$, on account of the logarithmic factor in the denominator, the curve is not quite

straight. This curve leads to path equations that are not integrable. If one were to adopt the second method mentioned above and consider this an instantaneous velocity, he would either have to use the log series, or substitute for the curve the nearest straight line. In the latter case he would commit himself to a doubtful approximation.

In Fig. 2 has been plotted also, in dashed line, an empirical velocity. This is an actual observed velocity, one that is well established and has been much used. This particular one was chosen merely because it is of a typical form. It will appear in subsequent figures. The constant A for each of the curves in Fig. 2 has been so adjusted that they all intersect the empirical velocity at the 7000 foot level, which point falls about in the middle of the reliable part of this velocity. It will be noted that a value of n between 6 and 7 would give a pretty good fit to the empirical velocity—beyond a certain point, which in this case lies at about the 4000 foot level. Between this point and the surface it is obvious that no curve of this type could fit the given velocity at all. Since every empirical velocity starts with a fairly high initial value, there will always be, for this type of curve a gap within which the curve is rising from zero to meet the given velocity.

It may be objected that since most empirical velocities are not well determined or perhaps not determined at all for the shallow depths, it is quite unimportant whether the mathematical curve fits well in this region or not, so long as it fits well at the greater depths. But, as already pointed out, it is precisely at the shallow depths that corrections for curvature are required. A little consideration will show that reflections from the most steeply dipping surfaces, as from the side of a fault, can be obtained only at shallow depths. Suppose, for instance, that the side of a fault is inclined 60° to the horizontal and lies at a depth of 10,000 feet. For a seismic ray to reach this fault and be reflected back to the neighborhood of the shot point, the fault would have to lie at a horizontal distance from the latter of about 17,000 feet. The total length of the ray paths would be about 40,000 feet. For the steepest dips, then, the reflecting beds must lie near the surface. If the empirical velocities are not reliable for the shallow depths, the remedy is to improve them.

This type of velocity law has been applied by Blondeau in a special method of computing the weathering time. He argued persuasively that since the surface velocity is very low, sometimes as low as 700 feet per second, whereas at a depth of 100 feet or so it will have increased to several thousand feet per second, very little error is com-

mitted in assuming the surface velocity to be zero. This is undoubtedly true, and since the whole weathering time is only a small fraction of the reflection time, a fairly large error in the former is still only a small error in the latter. But the argument doesn't hold for a ray that starts with an initial velocity of already several thousand feet per second, and in a further depth of 10,000 feet gains only two or three thousand feet per second. Here the initial velocity is no longer a negligible quantity.

Another objection to this type of velocity law is that the ray paths to which it leads all start vertically downward, no matter where they come up. It is impossible, therefore to distinguish one ray from another, or to tell where it comes up, by means of any characteristic that can be discerned at the shot point, such as the starting angle. The starting angle for all of them is 90°, and likewise the emergent angle. Now, while such rays are mathematically possible, they are physically impossible, An actual ray that starts vertically downward, continues unswervingly on that course, and never bends around and returns to the surface. At the point of the explosion, rays start out in *all* directions, and where a particular ray comes up depends on its starting angle.

For all of these reasons, equations of type I, the parabolic family without initial velocity, are wholly unsuitable for the calculation of ray paths.

II. A considerable improvement is effected by providing the equations of type I with an initial velocity. The general equation then becomes

$$V = V_0 + Az^{1/n},$$

which is type II. The effect is merely to raise the curves of Fig. 1 through the vertical height V_0. They are hence all of the same form as before; they merely start from an elevated point. In consequence of this they can be better fitted to an empirical velocity. The gap at the shallow depths is reduced. All of these curves, as before, lead to path equations that can be integrated by elementary means when n is an integer. But a new difficulty arises when an equation of this form is converted to the corresponding average velocity relation, which is the one that must be fitted to the empirical velocity.

Fig. 3 shows the instantaneous and the average velocity curves and their equations for $n=1$. The former is of course a straight line. The latter is nearly straight, but is modified by a logarithmic factor in

the denominator. On account of this factor it is very difficult to fit this curve to the empirical velocity. The equation can be solved only for V_0, not for A. This makes it very difficult to apply least squares in adjusting the constants. One could, of course, replace the slightly curved average velocity line by the nearest straight line. But the figure shows that even the best straight line would be a poorer fit than the curve.

This linear variation of velocity with the depth has always been a

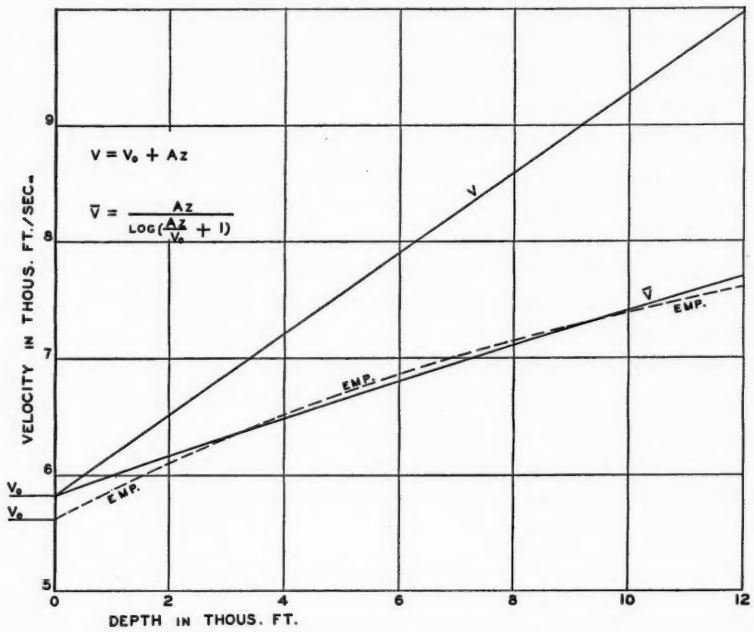

FIG. 3.

favorite with the mathematicians. It is the simplest imaginable case and very easy to work out. As is well known, the corresponding seismic paths are arcs of circles whose centers lie on a horizontal line at a height above the ground that is given by the intercept of the instantaneous velocity curve with the Z axis. All the problems involved can be solved by pure geometry.

Fig. 4 shows the curves and their equations for $n = 2$. The equation for the average velocity is more complicated than before, and now cannot be solved for either V_0 or A. The application of least squares

is out of the question. Nevertheless, the figure shows that a good fit to the given empirical velocity can be obtained—if one cares to spend the time. A better fit might be obtained for $n=3$, but the average velocity equation then contains one more term, and so on. The labor of fitting the equations for these higher values of n is certainly prohibitive.

For all of these curves, except when $n=1$, the V_0 for the curve

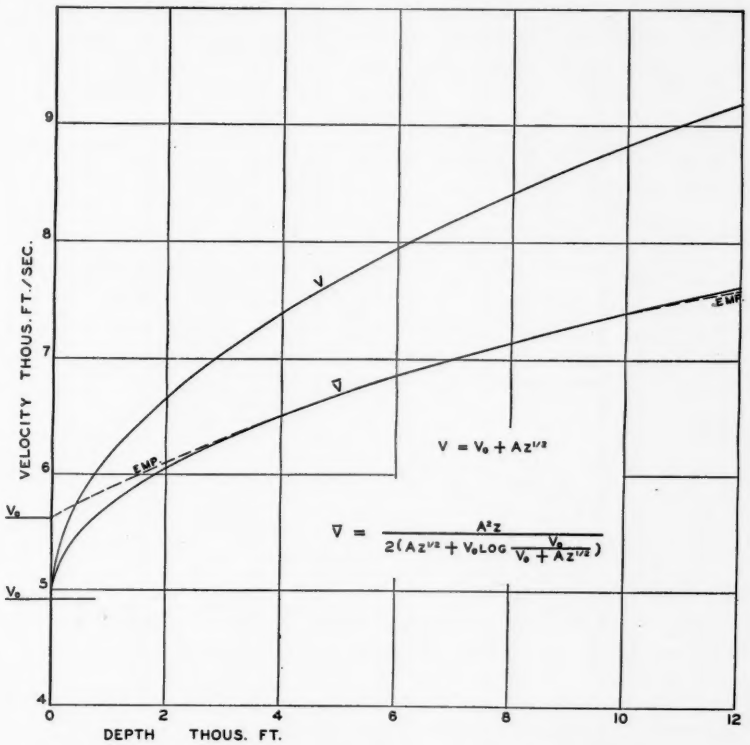

FIG. 4.

must, for good fit, be less than the empirical initial velocity. Hence there is still a gap for the shallow depths, but it is smaller in extent and the amount of the misfit is reduced. When $n=1$, the V_0 of the curve must be greater than the empirical initial velocity, and the misfit is in the other direction.

Because for all of these curves there still exists a gap, and because of the difficulties of fitting them to an empirical velocity, they must all

be discarded with the possible exception of the case where $n=1$. But this last must also be discarded for other reasons.

A linear variation of velocity with the depth is much too rapid. This is strikingly shown if one calculates and plots the corresponding

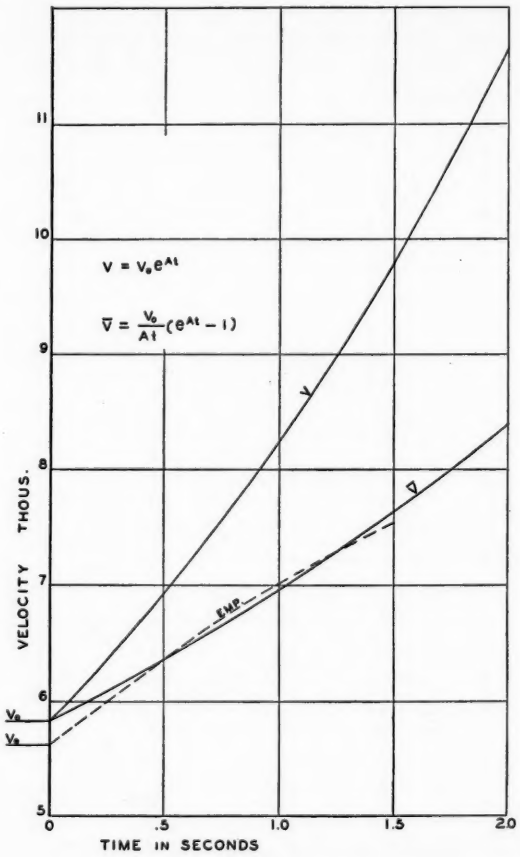

FIG. 5.

velocity-time curves. These and their equations are shown in Fig. 5. It is seen that they are exponential. The velocity increases with the time at a continually increasing rate, like compound interest, and eventually reaches infinity. No actual velocity ever takes such an exponential joy-ride.

Of course one does not expect an empirical velocity to follow such

a curve to the absurd extremes, but only for a little ways along the lower end where the slope is gentle and the curvature is mild. But even so it is difficult to find an empirical velocity that curves upward throughout its whole length. It may be concave upward for a short piece, but eventually becomes convex. An entirely different sort of equation is required to fit such a curve, and leads to path equations that cannot be integrated.

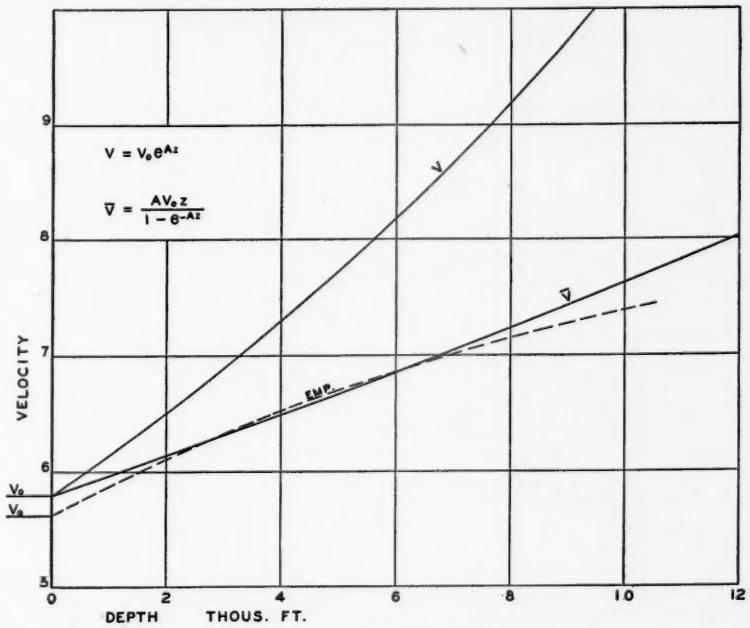

FIG. 6.

III. Fig. 6 shows the curves of type III, an exponential variation of velocity with the depth. The instantaneous velocity is of exactly the same form as in Figure 5; z is merely substituted for t. The average velocity is a little simpler. This exponential law is also a mathematician's delight, not only because it is so easy to work out, but also a little perhaps because it looks quite impressive. But if a linear variation of velocity with the depth was too rapid, so much the more so is an exponential variation. The corresponding velocity-time curves, Fig. 7, shoot up still more explosively. But this is not the worst. Both velocities reach infinity within a *finite* time. One would naturally suppose that this time would be something far beyond anything that

could be recorded on the geophones. But this is not the case. For the values of the constants required to bring the average velocity curve into proximity with the empirical velocity, this time turns out to be just three seconds.

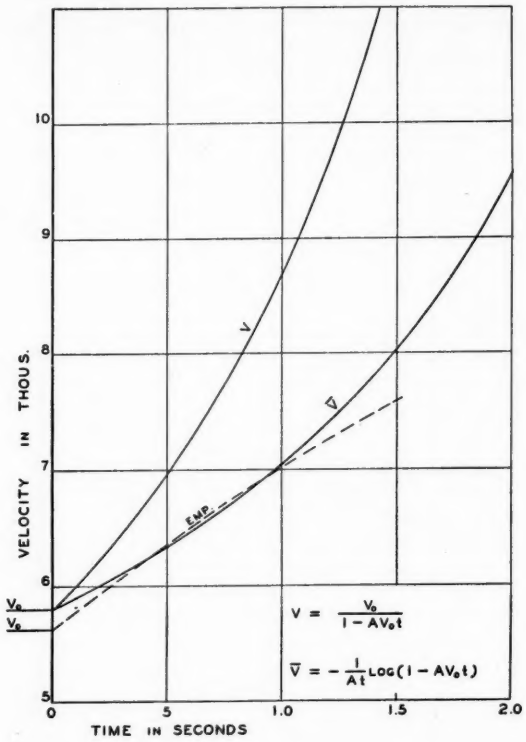

FIG. 7.

To show the nature of these curves more fully they have been drawn on a smaller scale in Fig. 8. Both curves approach the asymptote, $t=3$. The instantaneous velocity having reached infinity then suddenly switches to minus infinity. As t increases, this velocity rises along the dashed curve in the fourth quadrant, which is the negative branch of the hyperbola, and approaches the Z axis. The latter is another asymptote to both curves.

According to this law, for a depth of 12,000 feet, the average velocity is about 8000 feet per second. A reflection from this depth would therefore be received by the geophones about three seconds after the

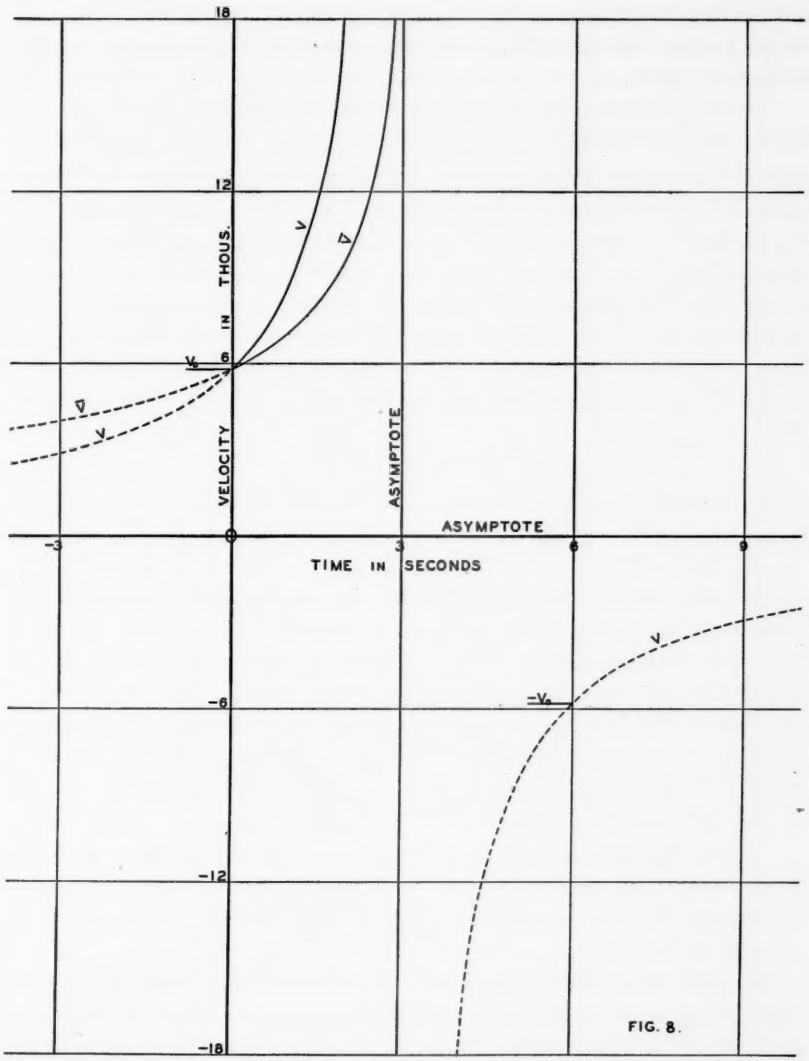

FIG. 8.

shot was fired. But if the reflecting surface were at the center of the earth, or even a million miles down, the seismic impulse would still return to the surface in less than six seconds. One can imagine how little accuracy could be obtained for the deeper beds.

The negative branch of the average velocity hyperbola is imagi-

nary—very much so, for the whole thing may be said to be imaginary. It is just a mathematical plaything, having no connection with seismic realities.

Having now rejected all the easily integrated velocity-depth laws, what is there left to do? Is one condemned to use the more complicated relations that can only be integrated by means of infinite series? By no means! Corresponding to the three types of velocity-depth laws discussed above, there are three types of velocity-*time* laws, which are obtained from the former by merely substituting t for z. The first and third of these would have to be immediately rejected for the same reasons that the corresponding velocity-depth laws were rejected. This leaves available only the middle group, the parabolic velocity-time law with initial velocity. Its general equation is:

$$V = V_0 + At^{1/n}$$

and the corresponding average velocity equation is:

$$\bar{V} = V_0 + nAt^{1/n}/(n + 1).$$

It is just as feasible to derive the path equations from a velocity-time law as from a velocity-depth law, and there are many advantages in doing so. One could of course convert to the corresponding velocity-depth law and proceed in the accustomed manner. But the latter is, for this group, one degree higher than the original velocity-time law. And almost in general, the derived depth relation is more complicated than the original time relation. It is better of course to use the simpler of the two relations in deriving the curved paths.

All of the equations of this group lead to path equations that can be integrated by elementary methods so long as n is an integer, and which are simpler than those derived from the like depth laws one degree higher.

In using the velocity-time in place of the velocity-depth relation, one is in general nearer the original observations, which is important from the point of view of numerical accuracy. Except in the more or less rare instance where an oil well is available to determine the depths, velocity measurements depend mostly on time observations. The only distances used are measured along the ground. The depths are calculated from these and the time measurements. They are not observed.

It will be noted that the average velocity equation above differs from the instantaneous velocity equation only in the value of the

constant coefficient. This case is hence as simple as the parabolic depth law which lacked an initial velocity. But these equations *have* an initial velocity. Least squares can be used in a simple way to fit any of these equations to a given empirical velocity.

Furthermore, if the fit is good on the velocity-time plot, it will be better on the velocity-depth plot, except when $n = 1$, in which case the fit is only just as good. This rule is quite general. It is noticeable in some of the cases already discussed, particularly in that of the

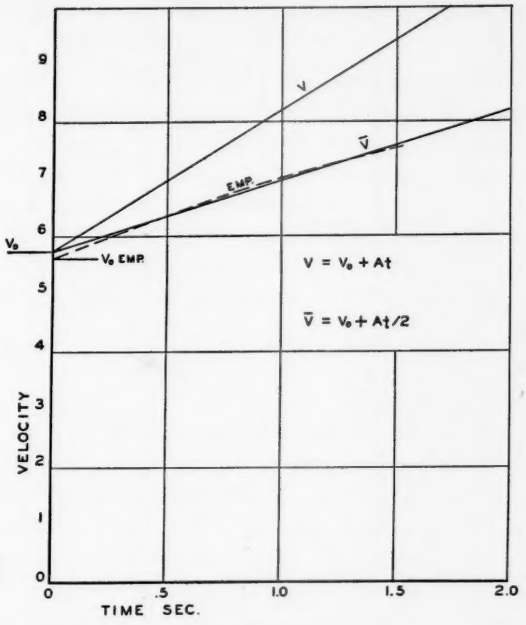

FIG. 9.

linear depth relation. On the velocity-depth plot the mathematical curve could be fitted after a fashion to the empirical curve, because both were convex. But on the time plot they could not be fitted at all, because one was convex, the other concave. The time plot is, so to speak, the more sensitive, and is therefore the one on which the fitting should be done.

Finally, this type of equation gives a better fit than any of those so far discussed, as will now be shown.

Fig. 9 gives the simplest example of this group, the linear variation of velocity with the time. The average velocity is also a straight line,

and its constant is merely half that of the instantaneous velocity equation. This makes it extremely simple to fit to any empirical velocity that can be adequately represented by a straight line. The fit in the figure is not very good at the shallow end only because there were no observations at this end. The curve drawn is an eye extrapolation at this end. The line was fitted, by least squares, only to the reliable part of the curve, and for this part the maximum deviation is about 50 feet per second.

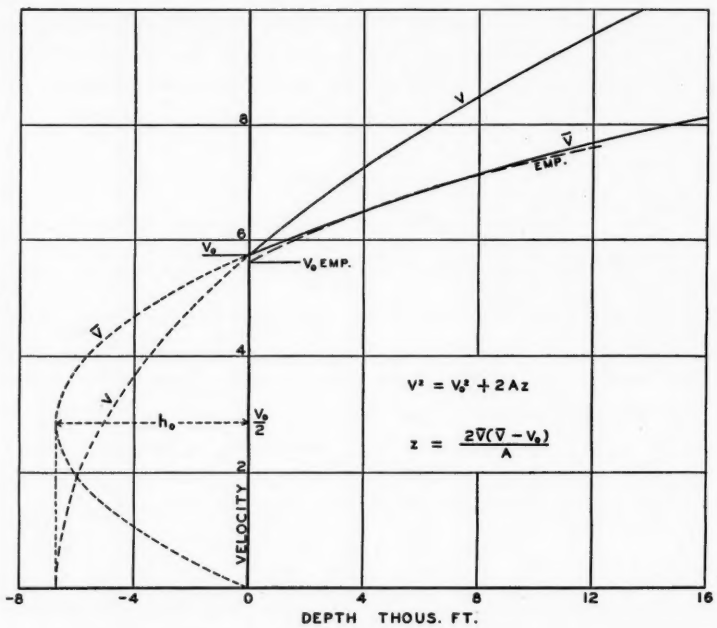

FIG. 10.

Fig. 10 shows the corresponding velocity-depth curves. In practice, as already stated, it is not necessary to make this plot, which is here shown only for illustration. Both curves are second degree parabolas. The instantaneous velocity curve has its vertex on the Z axis at a distance, which has been designated h_0, *behind* the V axis. The average velocity curve has its vertex at the same distance behind the V axis, but at the height $V_0/2$. As a consequence of this, the empirical curve can be fitted throughout its entire length, just as well at the shallow as at the deeper end, provided of course there are observations that justify a close fit at the shallow end, which in this

case there were not. At any rate, there is no *necessary* gap at the shallow end as there was for the parabolic depth curves of Fig. 4. Here, all the sharply curved part of the parabola lies behind the V axis instead of in front of it, in the unused instead of in the used part of the diagram. The curve rises to the proper height and takes the proper slant before reaching the zero hour.

The seismic paths to which this linear velocity-time relation leads are also quite simple. They are cycloids generated by a circle that rolls on the under side of a horizontal line at the height h_0 above the ground. There is hence a certain analogy between this case and the linear velocity-depth case.

All the curves of this class have the advantages mentioned. There is no necessary gap at the shallow end for any of them. All can be easily fitted, and are not too difficult to handle. Since their forms and properties are much the same as those of the curves shown in Fig. 10, it is needless to discuss them in detail.

Some of the more complicated curves, such as the S shaped ones, remain yet to be investigated.

When the seismic paths and the wave fronts are once obtained, there are two ways of using them. Either the dips and depths may be directly derived from them, or corrections may be drawn up and applied to the dips and depths calculated on the straight line assumption. The former method would be ideal if by means of tables or charts it could be made nearly as simple as the straight line method, and if the mathematical curve could always be fitted closely to the empirical velocity. But, at the present time, the last requirement cannot always be met. If the fit is poor, it is obvious that the errors of the fit will appear directly in the results. When the fit is not sufficiently good for the first method, then the second method must be applied. It is true that the errors of the fit will similarly affect the corrections that are calculated, but since the main part of the dips and depths calculated on the straight line assumption are based on the original empirical velocity, the errors of the misfit, affecting only the corrections to be applied, will affect the final results to a far less extent.

This paper has dealt only with theoretical aspects of the subject. It is hoped in a later paper to deal with some of the practical applications.

INTERPRETATION OF WELL-SHOT DATA*

C. H. DIX†

ABSTRACT

A method of interpreting well-shot data is presented having the advantage that the velocity distribution calculated can be made to fit the data with any desired closeness. In practise, the method is not difficult to apply. With discrete data, a unique interpretation evidently cannot be given, but in the case of ideal data, including also surface refraction data, the velocity distribution is uniquely determined.

INTRODUCTION

Most exploration geophysicists are familiar with the problem treated here, namely, that of determining the distribution of seismic velocity, v, with the depth h, by well-shooting. The problem has been previously treated by Slotnick,[1] without, however, more than illustrating particular cases. Essentially, the problems solved by Slotnick are: given data from either linear or exponential distributions, find the particular linear or exponential distributions. It appears to the author that the real problem confronting the interpreter of the data is, on the other hand: *given the well-shot data, find the relation between v and h.*

Unfortunately, the data are not perfect, being given at only a discrete set of values of h and subject to error of measurement at each of these depths. Also, the hypothesis we are forced to make concerning the sole dependence of v on h is seldom exactly met with in nature, at least in an oil well, where every effort has been made to base drilling on the negation of this hypothesis.

However, the method outlined in this paper should prove of considerable practical value, as it gives a direct process for finding $v(h)$, which fits the data within the range of the probable error. We work through an example in which the real $v(h)$ is known. In fact, we made up the data from $v=v_0(1+kh)$, with $v_0=2000$ meters per second, and $k=.0005$. Our results, so far as $v(h)$ is concerned, do not come very close to $v=2000(1+.0005h)$. The reason for this is pointed out in the example. However, reflection depths calculated on the basis of our interpretation will be very good approximations to the facts. Actual

* Paper received Oct. 29, 1938. Read at Geophysical Research Conference, California Institute of Technology, May, 1938.

† Pasadena, California.

[1] M. M. Slotnick, GEOPHYSICS, vol. I, no. 1, pp. 9–22, and vol. I, no. 3, pp. 299–305.

cases will sometimes furnish better examples, since they often contain large sudden changes in velocity, which render the average velocity method inaccurate at just those levels where it is used.

PRINCIPLE OF THE METHOD

Let $t(x,h)$ be the travel-time from the source to a point a depth h below a surface-point a distance x from the source or shot-point. The curves

$$t(x, h) = \text{const.}$$

represent the wave-fronts. Now the directional derivative of $t(x,h)$ in the direction normal to the wave-fronts is

$$dt/dn = |\operatorname{grad} t| = [(\partial t/\partial x)^2 + (\partial t/\partial h)^2]^{1/2} = 1/v(h). \qquad (1)$$

This equation is fundamental to our work. We write it in the form

$$t_x^2(h) = 1/v^2(h) - t_h^2(h), \qquad (2)$$

in which the subscripts indicate corresponding partial differentiation; i.e., for example

$$t_x(h) = \partial t(h)/\partial x.$$

Obviously

$$t_x(h) = \sin i_0(h)/v(0) = p(h) \qquad (3)$$

where $i_0(h)$ is the angle between the downward vertical and the forward tangent to that particular ray that passes through (x,h). Evidently, knowing t_x by shooting from two shot-points, we can determine $v(h)$. However, it is unnecessary to shoot from two shot-points.

Let us examine the effect of a discontinuity of $v(h)$ on t_h. If we allow i_0 to decrease slowly, the corresponding values of h, swept out by the rays on the well, will sometimes be increasing and sometimes decreasing, so that t_x may be a multiple valued function of h. However, t_x, on any one of its branches, is a continuous function of h. Hence, if $v(h)$ has a discontinuity, then t_h must have a corresponding one, and conversely.

Let $f(h+0) = \lim_{\epsilon \to 0} f(h+\epsilon)$, and $f(h-0) = \lim_{\epsilon \to 0} f(h-\epsilon)$, where $\epsilon \geqq 0$. Then

$$p^2(h+0) - p^2(h-0) = 0 = 1/v^2(h+0) - 1/v^2(h-0) - t_h^2(h+0) + t_h^2(h-0)$$

or

$$1/v^2(h+0) = 1/v^2(h-0) + \Delta(t_h^2(h)). \qquad (4)$$

Thus, if the (t,h)-curve has a corner at h_1, the corresponding $\Delta(t_h^2(h_1))$ measures how much the discontinuity in v is by (4).

We shall suppose that our data is given by

$$t(\zeta, 0), \qquad 0 < \zeta < 2x, \qquad \text{(Refraction Data)},$$
$$t(x, \xi), \qquad 0 < \xi < H, \qquad \text{(Well Data)}.$$

t may be multiple valued as a function of ζ for $h=0$, and may show a finite number of discontinuities. t may be multiple valued as a function of ξ and on each branch is continuous. We suppose that $t_\xi(x,\xi)$ is given on each branch, and on each branch has only a finite set of discontinuities.

We can divide the interval from 0 to H into a finite set of sub-intervals in the following manner: If the refraction data shows that $v(\xi)$ is increasing down to a certain depth, h_1 (corresponding to the first discontinuity in the refraction data), then the first interval is $(0,h_1)$. In such a case, $t_\xi(x,\xi) \leqq 0$ in $(0,h_1)$. If $v(\xi)$ is non-increasing at $\xi=0$, then $t_\xi(x,0)=0$ and $t_\xi(x,\xi)>0$ in the interval $0<\xi<h_1$, and $t_\xi(x,h_1)=0$. In the first case, refraction data is used to compute $v(\xi)$ in $(0,h_1)$. In the second case, the well data is used in $(0,h_1)$. In the first case, $v(\xi)$ will be non-increasing below h_1, and consequently there is a branch of the (t,ξ) curve starting at $\xi=h_1$, such that $t_\xi>0$ until a depth h_2 is reached. If there are several such branches, we may choose the one that makes h_2 a maximum. At h_2 we have either reached H or else $t_\xi(x,h_2)=0$. In the second case, v may increase or not-increase in an interval below h_1. If v does not-increase, v may be computed down to h_2 from the well data, where h_2 is either H or the next place where $t_\xi=0$. If v is increasing at h_1+0, surface refraction data can be used down to h_2 which will correspond either to a turning point of v or else to the next place where $t_\xi=0$ or to H.

We proceed in the above manner until $(0,H)$ is covered. This will always be possible if v has only a finite number of turning points.

In an interval where $t_\xi \leqq 0$, refraction data is interpreted following Schlichter.[2] In the case where $t_\xi>0$ in an interval, we adopt the following method.

METHOD FOR CASE $t_h>0$. UNIQUENESS

In such an interval on one branch of the data, we have

$$t(x, h) = \int_0^h \frac{d\xi}{v(\xi)(1 - p^2(h)v^2(\xi))^{1/2}} \tag{5}$$

$$x = \int_0^h \frac{p(h)v(\xi)d\xi}{(1 - p^2(h)v^2(\xi))^{1/2}}. \tag{6}$$

[2] L. B. Schlichter, *Physics* 3, p. 274 (1932).

Let the interval be (h_i,h_{i+1}). $v(h_i)$ and $p(h_i)$ are known. Suppose $\bar{p}(h)$, $\bar{v}(h)$ form a solution of (5) and (6) on the branch of the data under consideration.

Now, if $\bar{p}(h_i)>p(h_i)$, evidently $\bar{x}>x$, where

$$\bar{x}=\int_0^{h_i}\frac{\bar{p}\bar{v}d\xi}{(1-\bar{p}^2\bar{v}^2)^{1/2}} \qquad \text{and} \qquad x=\int_0^{h_i}\frac{pvd\xi}{(1-p^2v^2)^{1/2}}.$$

Now $p(h)$ and $\bar{p}(h)$ are monotone non-increasing functions of h in (h_i,h_{i+1}), and $p(h_i)=\bar{p}(h_i)$. If $p(h)=\bar{p}(h)$ in an interval (h_i,h_{i+1}), then $v(h)=\bar{v}(h)$ in this same interval by (2) and (3). If, however, $p(h)>\bar{p}(h)$ in (h_i,h_{i+1}) except at h_i, then $v(h)<\bar{v}(h)$ except at h_i. This is evidently impossible, since even over the path given by $v(h)$, the travel-time is shorter with the $\bar{v}$ distribution than with the v distribution. Hence minimum travel-times over the $\bar{v}$ distribution are shorter than minimum travel-times over the v distribution, which is impossible, since the data are fixed.

The above argument may be applied to show that there is no sub-interval in (h_i,h_{i+1}) where $p>\bar{p}$. By interchanging p and $\bar{p}$, we see that $\bar{p}>p$ likewise leads to a contradiction of the data. Hence, $v(h)=\bar{v}(h)$ in (h_i,h_{i+1}). *Thus $t(x,h)$ uniquely determines $v(h)$ in an interval where $t_h>0$.*

APPROXIMATE CALCULATION FOR CASE $t_h>0$

We divide up (h_i,h_{i+1}), so that $h_i=0_i$, $h_{i+1}=n_i$, and the division points are 1_i, 2_i, $\cdots$, $(n-1)_i$, thus giving n intervals. We know $v(h_i-0)=v(0_i-0)$, and can find by (4) what $v(0_i+0)$ is. Let $v'=v(0_i+0)$ in $(0_i,1_i)$. This will lead to $t'(x,h)$. The approximate value of p will be known from the top to the bottom of the interval. Also, $t_h'(x,1_i-0)$ is known. Form $t_h'(x,1_i+0)=\frac{1}{2}[t(x,(1_i+2_i)/2)-t'(x,1_i-0)/](2_i-1_i)$. Then we can compute $\Delta t_h'^2(x,1_i)$, and hence $v(1_i+0)$. Carry this down until (h_i,h_{i+1}) is covered.

Note that in each layer, since v is constant and p is decreasing, t_h' is increasing so that the t' curve is a series of scallops. There are two ways of bettering the approximation. One is, to make better agreement between t_h and t_h'. The other is, to increase n. It will be found that if, in any interval, a value is given much different from that which follows the t and t_h closely, a large swing to the other side of the data will be generated. It will also be found that this oscillation can always be reduced, if the t_h data suggests a reduction. A method of reduction is the following: (1) at 1_i, we have $t'(x,1_i)\gtreqless t(x,1_i)$;

(2) thus $v'(1_i-0)$ is respectively too small, correct, or too large; (3) choose values respectively larger than, the same, or smaller than, $v'(1_i-0)$ for $v''(1_i-0)$, and compute the corresponding $t''(x,1_i)$; (4) thus from t'', t', t, and v', v'', we can, by interpolation or extrapolation, compute a v''' which will give a t''', closer to t than t' or t''; (5) then compute t_h', using the mid-point of the next interval and t''', and again make the adjustment as described in (1), (2), (3), and (4).

That this process converges is evident if we impose a sufficient set of restrictions upon t and its derivatives. Since data in practice never require us to go further than to introduce a few corners in the curve for t, we feel justified in stopping the general mathematical part of this paper here.

APPLICATION TO AN EXAMPLE

Suppose we have a shot-point 500 meters away from the well-top, and we take a record of the travel-time at the top and every 100 meters, down to 1000 meters. Our data are then plotted on Fig. 1. There is nothing in the data opposed to a linear distribution down to where $t_h=0$. This appears to be at about 70 meters. Since the travel-time to $h=100$ meters is .245, and likely that to 70 meters is slightly less, let us guess it at .244 sec. Then the travel-time to the point 1000 meters from the shot-point and 500 meters from the well-mouth is .488 sec. Thus we have three points for our surface refraction data, namely: (0,0), ($x=500$, $t=.250$), and ($x=1000$, $t=.488$). In the interval (0,500), .250 sec. corresponds to 2000 m./sec. In the interval (500,1000), $.488-.250=.238$ sec., corresponds to 2100 m./sec. If we assume then, $v(0)=2000$ m./sec. and $v(70)=2100$ m./sec., we get $k=(1/v(0))(dv/dh)=.0007$ approximately. One may now construct several circular arc rays and wave-fronts, and, to a sufficiently good approximation, calculate times on the wave-fronts from their intersection with $h=0$, considering the velocity along the surface to be 2000 m./sec. We find that the fit thus obtained is sufficiently good down to $h=150$ m., but at 250 m. there is too much divergence. We therefore stop the linear distribution at 150 m. We need to know the angles of incidence of the rays striking the 150 m. depth as well as the travel-times to points at this depth. These can readily be found by drawing in a set of rays and wave-fronts, and plotting the values measured. The times are represented by curve T_1 on Fig. 2. The angles are given by i_1 on Fig. 3. The construction sheet is Fig. 4. Having i_1

at each point of $h=150$, we need next the change in velocity. $v(150)=2000(1+.0007\times150)=2210$ m./sec. By placing a pair of triangles on the data, t_h can be determined in the same way as apparent velocity is determined in refraction computing. I find

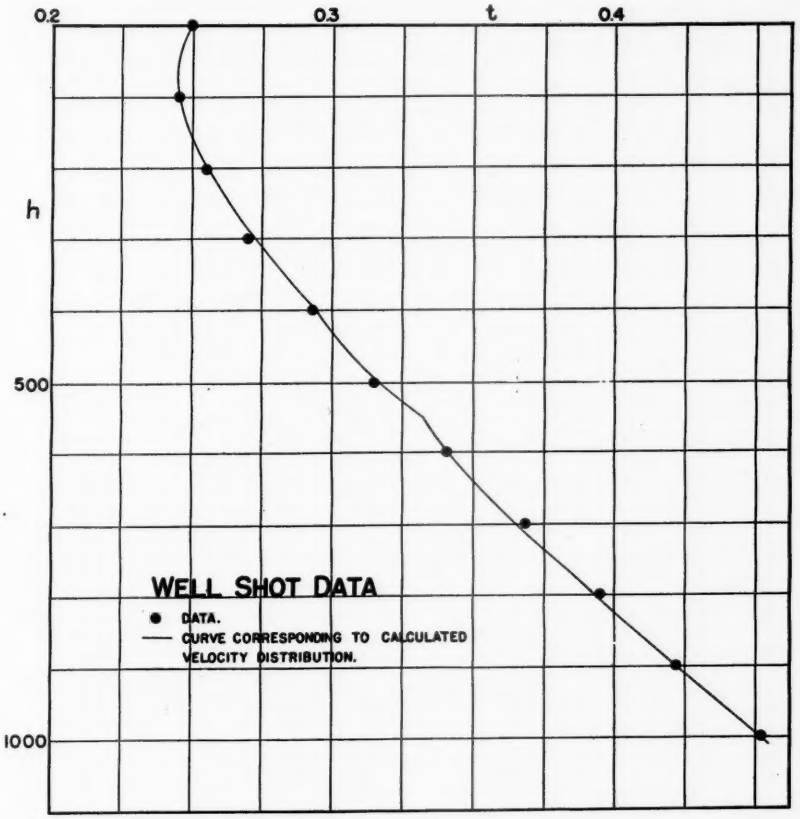

FIG. 1.

$t_h(150-0)=.9\times10^{-4}$, and $t_h(150+0)=1.5\times10^{-4}$. Thus $t_h^2(150-0)=.81\times10^{-8}$, $t_h^2(150+0)=2.25\times10^{-8}$, and $\Delta t_h^2(150)=1.44\times10^{-8}$. Hence, by the application of (3), we get $v(150+0)=2135$ m./sec. Applying Snell's law, we find that the sines of i_1's, multiplied by 2135/2210, give the sines of corresponding r_1's, and hence the r_1 curve can be drawn as shown on Fig. 3. The travel-times, T_2, to points on

$h=250$, are readily found on the construction sheet and graphed on Fig. 2. $\Delta t_h^2(250)$ is found to be -1.85×10^{-8}, which makes $v(250+0)$ $=2230$ m./sec. Thus r_2 can be graphed, and the times carried down another step. In this way, the whole of the data can be fitted.

It may be observed that at a depth of 545 m. a point has been allowed that falls off the smooth curve but not off the data. The fit has been maintained, however, by suddenly increasing the velocity

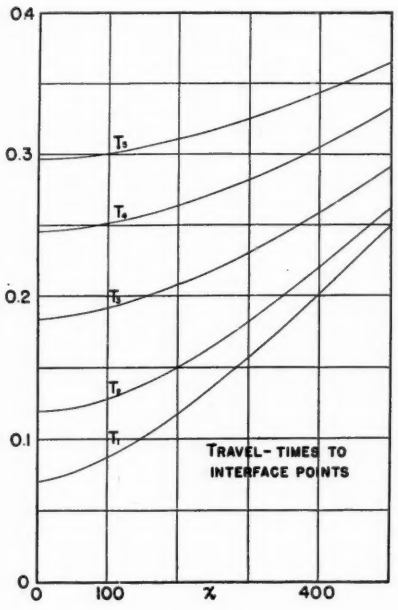

FIG. 2.

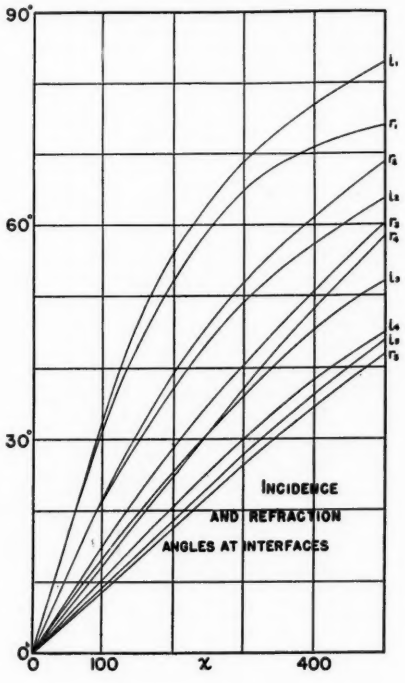

FIG. 3.

to 2950 at 550 m. Such an irregularity could have been avoided by making the break at 500 meters. Note that the smoothness of the curve is determined by the magnitude of the Δt_h^2's. If sudden changes of v are indicated by data, then Δt_h^2 may be allowed to be large correspondingly. If, however, the data indicates smoothness of the v distribution, Δt_h^2's must be held down by making more frequent and smaller changes in velocity, or by holding more closely to the smooth curve.

CONCLUSION

Considering the large expense involved in obtaining the present well-shot data, it appears to the author that the velocity logs should

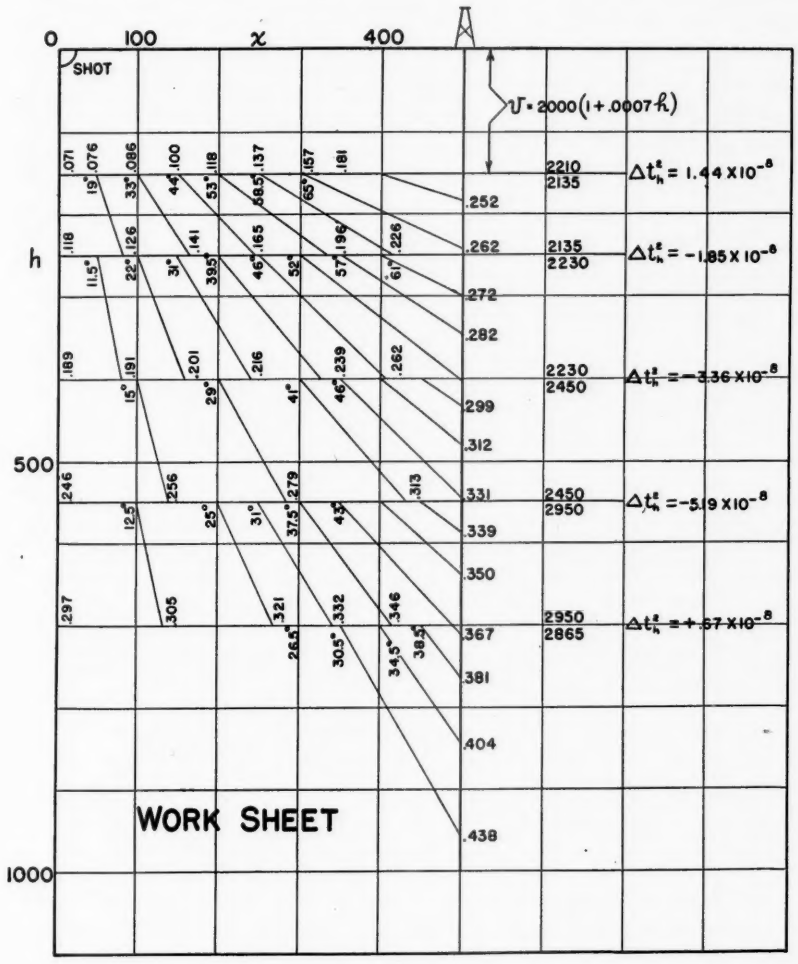

FIG. 4.

be obtained so as to fit all possible data as closely as possible. The author recalls a case of a well in an important area, where very deep reflections were recorded in addition to two good shallow reflections. Could these deeper reflections be multiple reflections? By computing

the two shallow depths and the velocity log at the well, it was found that the deeper (?) reflections corresponded closely with the multiple computations. The author believes that this lends strong support to the multiple reflection interpretation. Besides the evident theoretical interest, is the practical interest in weighing the evidence for and against drilling on structures that may be true deep structures and may be merely the result of multiple reflections.

Referring back to Slotnick's work, it is to be observed that in many large areas linear distributions are in excellent agreement with all available data. In such cases the present method is unnecessarily laborious and Slotnick's graphs furnish a convenient means of interpreting the data.

STEADY STATE POLAR SENSITIVITY CURVES*

C. H. JOHNSON†

ABSTRACT

The resultant amplitude, "A," of the combined outputs of a group of geophones is derived as a function of the difference in time of arrival, ΔT, at extreme geophones in the group—the number of geophones and the period of the waves being parameters. "A" plotted as a function of ΔT is shown to have principal and secondary maxima whose amplitudes, separation, and sharpness are discussed. The relative response of the geophone group to waves from every direction is considered and illustrated by polar sensitivity curves. The changes in the polar sensitivity curves effected by changes in the number of geophones, the geophone spread, or the wave length, are considered. The effect of introducing artificially controlled time differences between geophone outputs, so as to vary the direction of maximum response (so-called variable compounding) as is done in the Rieber Sonograph, is considered. By this means the resultant response of the group of geophones can be focused, so as to emphasize waves arriving from any specific direction. While the results are strictly applicable only to the case of steady state, sinusoidal waves, they may apply qualitatively to all the waves encountered in seismic exploration. The versatility of variable compounding is pointed out.

The reflection seismograph method of geophysical exploration depends for its success on clear recognition of reflected waves on a majority of the traces of the seismogram. Where other wave energy appears on the record, the reflected waves are masked and either cannot be seen at all or are so distorted that times of arrival or wave shapes cannot be trusted. The scope of the reflection method would be greatly extended if the desired reflection waves could be accentuated relative to the interfering waves.

To emphasize certain waves and suppress others arriving from the earth, use may be made of those properties wherein the waves to be separated differ. Some undesirable waves, such as gound roll and wind noises, may differ substantially in frequency from the desired reflection waves; in this case a segregation by means of frequency selective circuits is possible.

Waves also differ as to their angle of arrival at a point on the surface of the earth. This property enables them to be separated by means of directionally selective methods.

Since the surface stratum of the earth usually has a much lower velocity of propagation for elastic waves than the stratum immediately below it, waves arriving from a wide range of angles below

* Paper read at Annual Meeting, New Orleans, La., March, 15, 1938.

† Rieber Laboratory, Los Angeles, California.

the surface stratum are refracted into a narrow range of angles before reaching the surface. For this reason directionally sensitive geophones have been little used in commercial reflection seismograph practice. The tendency, instead, has been to interconnect several geophones to obtain a directional selectivity.

When geophones are so interconnected, the problem of determining the cumulated amplitude as a function of the direction of wave arrival is analogous to the optical problem of the diffraction grating[1] and to the problem of directive antenna arrays in short wave radio.[2]

Various phases of the geophysical problem have been treated by Born,[3] Rieber,[4] Klipsch,[5] McDermott,[6] Mott-Smith,[7] and the present writer.[8] Klipsch presented an excellent solution on the "assumption that all noise [should] be treated as irregular or random in its nature." The problem has not been followed through as completely for the assumption that an important part of the "noise" is composed of a finite number of regular wave fronts.

Klipsch remarks that the summation of a series of wave trains gives rise to a very complicated motion of the ground at any recorder, "the complexity rendering an analytical attack practically impossible." While we will not attempt to give a general solution here we will present a simplified problem in which the number and shape of the waves arriving at a group of geophones are predetermined. At a later time the problem will be extended to include more complex conditions.

The present paper considers only the case of a steady state sinusoidal wave reaching a horizontal line of uniformly spaced geophones whose outputs are to be added.

In the first section of the paper, the equations are derived and the graphs are discussed for the cumulated amplitude as a function of the number of geophones and as a function of the phase difference between the waves put out by the extreme geophones.

In the second section of the paper, the cumulated amplitude is plotted as a function of angle of arrival in the earth. The resulting curves may be called polar sensitivity curves for a direct summation of the outputs of a line of equally spaced geophones. The effects of varying the number of geophones and the ratio of the geophone spread to the wave length are discussed.

In the third section of the paper, the discussion is extended to the Sonograph[10] process where the outputs of the individual geophones

[1] Numbered superscripts refer to bibliography at the end of the paper.

are recorded as reproducible sound tracks and subsequently cumulated after the introduction of equal phase differences between the points of reproduction on adjacent sound tracks. The resulting polar curves represent the effective sensitivity of the Sonograph process as a function of angle of arrival in the earth and illustrate how, by this process, the polar may be pointed in any desired direction.

DERIVATION OF EQUATIONS

Beginning with the case in which the plane wave front of a sinusoidal wave arrives simultaneously at five geophones regularly spaced along a line at the surface of the earth, we may think of the electric

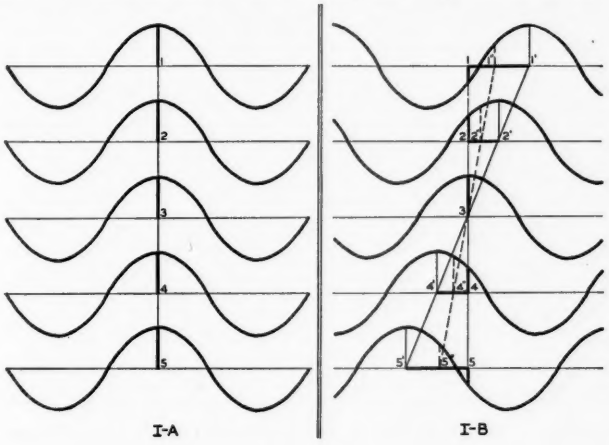

FIG. 1-A-B.

waves put out by the geophones, after steady state has been established, as the five sinusoidal waves of Fig. 1-A, recorded side by side on the customary seismogram, each wave representing the output of a single geophone.

In combining geophone outputs, various types of interconnection are employed, some involving only a partial exchange of electrical energy between the circuits following the geophones. However, only the case where all geophone outputs are added in their entirety will be treated here.

Directly adding the outputs from several geophones is equivalent to adding the waves of Fig. 1-A along vertical ordinates such as 1–5.

If the wave front does not reach the geophones simultaneously, the "seismogram" of single geophone outputs would appear somewhat like Fig. 1-B. A direct electrical addition of the waves put out by the

geophones would again be equivalent to adding the waves of Fig. 1-B along the vertical ordinates such as 1–5.

General theorems of sine wave addition indicate that if the waves of Fig. 1-A are added along the ordinates 1–5, passing through the maxima of the individual waves, the amplitude of the resultant cumulation will be obtained. Similarly if the waves of Fig. 1-B are added along the ordinates 1–5 the cumulative amplitude corresponding to a direct summation will be obtained.

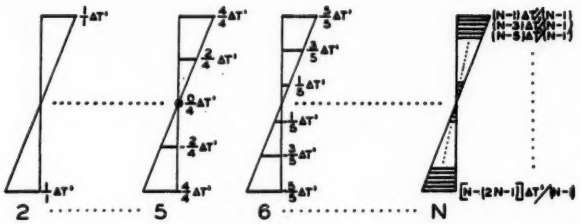

FIG. 2.

To determine the cumulative amplitude, A, as a function of the time difference, Δt, between extreme waves, and as a function of the number, N, of waves cumulated, we may define the figure formed by the crossing lines 1-5, 1′-5′ as a "phase figure." Figure. 2 shows a series of such phase figures for various numbers of waves cumulated. The time difference ($\Delta t/2$) between the top wave and the center wave has been called $\Delta t'$. The time differences between intermediate waves and the center wave are shown at the right of each "phase figure." The validity of the expressions for the phase differences for N waves is evident from a study of the series of figures.

If the equation for each wave is

$$y = \cos\left[2\pi(t + \Delta t')/T\right] \tag{1}$$

where t is time and T the period, the origin of time being at 3, then the cumulative amplitude, A, for five waves is

$$A = \cos\left(4\frac{\theta}{4}\right) + \cos\left(2\frac{\theta}{4}\right) + 1$$

$$+ \cos\left(-2\frac{\theta}{4}\right) + \cos\left(-4\frac{\theta}{4}\right)$$

where

$$\theta = 2\pi \frac{\Delta t'}{T} .$$

Similarly, for N waves

$$A = \sum_{s=1}^{s=N} \cos \left[(N + 1 - 2s)\theta/(N - 1)\right] \tag{2}$$

A is the real part of the series

$$S = \sum_{s=1}^{s=N} \exp^* \left[(N + 1 - 2s)j\theta/(N - 1)\right] \tag{3}$$

which is a geometric series. After taking its sum and rationalizing the denominator we have

$$S = \frac{(\exp j\theta + \exp -j\theta) - \left(\exp \frac{N+1}{N-1} j\theta + \exp -\frac{N+1}{N-1} j\theta\right)}{2 - \left(\exp \frac{2}{N-1} j\theta + \exp -\frac{2}{N-1} j\theta\right)} . \tag{4}$$

Since all these exponentials group into cosine functions, S has no imaginary part and equation (2) may therefore be regarded as a geometric series equal to S.

We may simplify (4), and obtain

$$A = \left(\sin \frac{N}{N-1}\theta\right) \Big/ \left(\sin \frac{1}{N-1}\theta\right) . \tag{5}$$

PLOTTING OF CURVES

It is instructive to plot the amplitude, A, as a function of the number of waves cumulated, N, and the total time difference, Δt, between extreme waves ($\Delta t = 2\Delta t'$). The family of curves is shown in Fig. 3.

Only a portion of each curve is shown. Each curve is symmetric about the A axis. If N is even, each curve repeats itself with a period of $2(N-1)$ on the $\Delta t/T$ axis. If N is odd, each curve repeats itself

* $\exp a = e^a$.

with a period of $(N-1)$. The amplitude of the principal maxima is N(or $-N$). Between the principal maxima there are $(N-2)$ smaller maxima which have amplitudes roughly $1/N$th of the amplitude of the principal maxima.

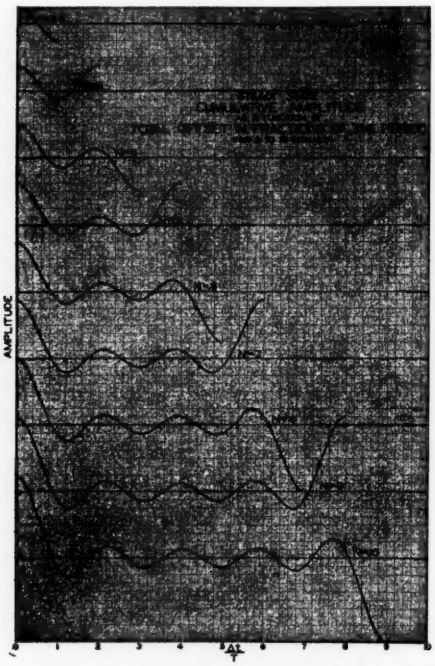

FIG. 3.

The roots are readily obtained from (5) but the exact positions of the small maxima are more difficult to determine. The values of θ for all maxima are given by:

$$\tan \frac{N}{N-1}\theta = N \tan \frac{1}{N-1}\theta \tag{6}$$

which may be solved graphically.

OPTIMUM NUMBER OF WAVES CUMULATED

Considering steady state sinusoidal waves, two factors influencing the choice of number of geophones connected together would be (1)

the sharpness of the "primary" maximum at zero Δt, and (2) the separation and size of the undesired maxima, either the equally large "secondary" maxima or the smaller, more numerous "tertiary" maxima.

To facilitate visualization of the first factor, the family of curves shown in Fig. 3 has been replotted in Fig. 4 with A/N as ordinates. Thus the amplitudes of all primary peaks reduce to unity, and it has been possible to add to the family the case where $N = \infty$.

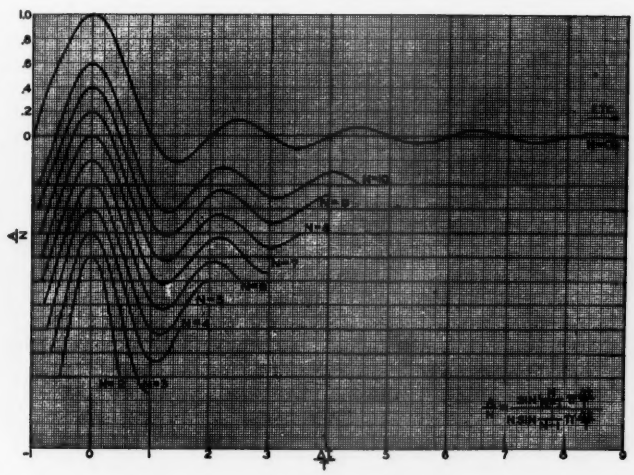

FIG. 4.

In order that the curves shall not intersect, each has been plotted on a $\Delta t/T$ axis slightly separated from that of its neighbors and has been plotted to the right only as far as its point or its axis of symmetry. Fig. 4 more nearly represents the results obtained when geophones are compounded than does Fig. 3, for an attempt is usually made to amplify all waves recorded in reflection shooting to as large an amplitude as can be conveniently read on the record, regardless of the amplitudes of the electric waves from the geophones.

Fig. 4 clearly shows an increase in the width of the primary maximum as N is increased.

Evidently, the wider the peak at some designated amplitude near its maximum, the less the sharpness. Thus, a reasonable definition of sharpness seems to be the reciprocal of this width.

The width, W_s, of the peak near the top is given by the expression

$$W_x = \frac{2}{\pi}\left[6 \frac{N-1}{N+1}(1-x) \right]^{1/2} \tag{7}$$

where x is the fraction of the primary amplitude at which the width is measured.

Setting $x=0.9$, we find for the width at that ordinate

$$W_{0.9} = 0.493[(N-1)/(N+1)]^{1/2}. \tag{8}$$

In Fig. 5 the sharpness, $1/W_{0.9}$, is plotted as a function of N, the number of waves cumulated. Evidently, while two waves should be

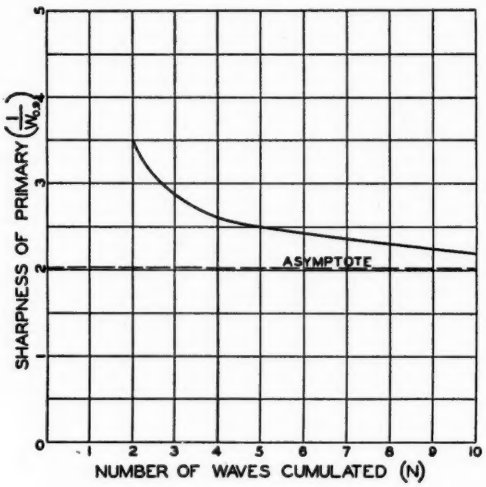

FIG. 5.

cumulated for maximum sharpness, there is no marked decrease in sharpness as N is increased above 3 or 4.

The second factor governing the choice of N, i.e., the effect of the irrelevant maxima, may be discussed in two parts. The secondary maxima are equal in size to the primary maximum (for steady state), but their separation from the primary is a function of N. The separation of the tertiary maxima is almost independent of N, but their average size is a function of N. These observations may be qualitatively verified by inspection of Figs. 3 and 4.

In Fig. 6 the separation of the first secondary maxima from the primary is plotted as a function of N. The equation for the curve is

$$\text{Separation} = N - 1 \tag{9}$$

obtained from (5).

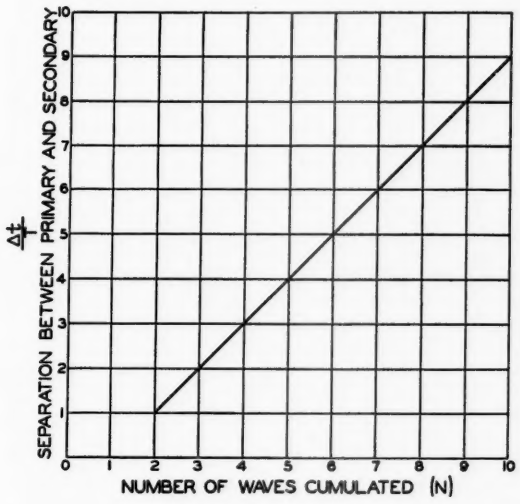

FIG. 6.

In Fig. 7 the ratio of the primary amplitude, A_p, to the mean tertiary amplitude, A_t, is plotted as a function of N. The curve, whose equation is not readily ascertainable, is obtained as follows:

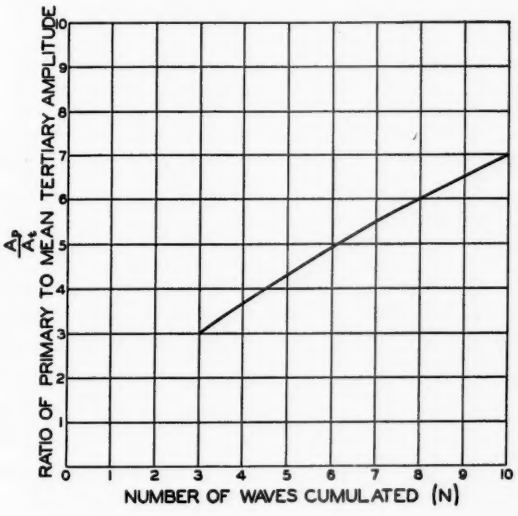

FIG. 7.

From (5) we may derive for each tertiary:

$$A_p/A_t = \frac{N \sin \frac{1}{N-1}\theta_t}{\sin \frac{N}{N-1}\theta_t} \tag{10}$$

where θ_t is the value of θ at which the tertiary maxima occur. This value of θ is obtained by solving (6) which may be done graphically by finding the intersections of the curves:

$$y = N \tan \frac{1}{N-1}\theta$$

$$y = \tan \frac{N}{N-1}\theta.$$

After the ratio A_p/A_t is calculated for each tertiary, the average for all tertiaries may be plotted as shown in Fig. 7.

From Figs. 6 and 7 it is clearly very desirable to increase N in order to minimize the effect of irrelevant maxima by

1. Increasing the separation between the primary and (large) secondary maxima,*
2. Increasing the ratio of the size of the primary maximum to the average size of the (small) tertiary maxima.

That the desirability of increasing N, as indicated by Figs. 6 and 7, far outweighs the undesirability, as indicated by Fig. 5, is demonstrated in the following discussion where the amplitude curves for cumulation are plotted as a function of angle of arrival at a line of N geophones planted in the earth.

POLAR SENSITIVITY CURVES FOR DIRECT ADDITION

Where the plane wave front reaches a group of geophones at the surface (neglecting the weathering correction) the angle, ψ, between its direction of arrival and the vertical may be represented by

$$\sin \psi = (\lambda/B)(\Delta t/T) \tag{11}$$

where λ is the effective wave length and B is the geophone spread.

* It should be remembered that we are discussing the artificial case of steady state sine waves. When a transient such as a damped sine wave is cumulated, both the secondary and the tertiary amplitudes are reduced. A discussion of this and other transient wave shapes will be presented in a future paper.

Eliminating $\Delta t/T$ between (11) and (5), and remembering that $\theta=\pi\Delta t/T$ we obtain

$$A = \sin\left(\frac{N}{N-1}\pi\frac{B}{\lambda}\sin\psi\right). \tag{12}$$

From (12) we may plot the amplitude, A, as a function of ψ, the angle of arrival in the earth, for various values of N, the number of geophones, and B/λ, the ratio of the geophone spread to the wave length. Fig. 8 shows a family of polar sensitivity curves for which $B/\lambda=5$ and N varies from 2 to 10.

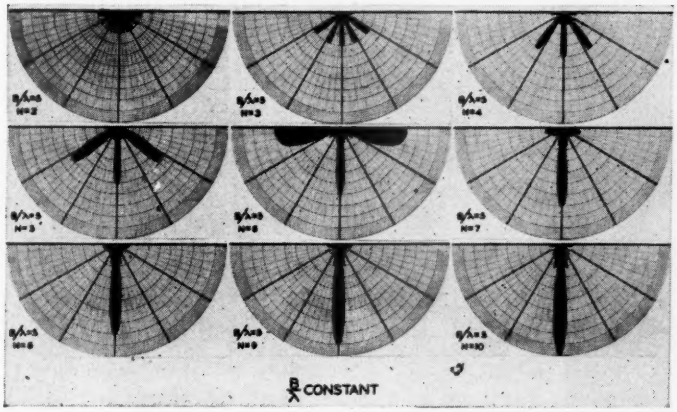

FIG. 8.

Here the ψ scale is the same for all values of N, just as the $\Delta t/T$ scale was the same for all values of N in Fig. 3. Thus it is evident that for a constant value of B/λ the sharpness of the vertical polar loop decreases as N is increased. (See also Fig. 5.) It should be noted, however, that there is a reduction of undesirable response loops as N is increased. (See also Figs. 6 and 7.) Evidently the advantages of increasing N outweigh the disadvantages.

Fig. 9 shows the effect of varying B/λ while keeping N constant. For this family of polars B/λ varies from 2 to 10 while N remains 10. We may conclude that for $N=10$, we may choose $B/\lambda=6$, 7, or 8 with almost equal sharpness and freedom from unwanted response loops. When B/λ is very small the primary response loop is fairly broad. When B/λ is very large, interfering response loops appear. In

case $B/\lambda = 10$ and $N = 10$, waves arriving at 60° from the vertical have the same amplitude as waves arriving vertically.

Apparently there is a value of B/λ corresponding to each value of N, which will yield the sharpest possible primary response loop without introducing "secondary" response loops of amplitude equal to the primary (for steady state). From equation (11) we see that when $\psi = 90°$, $B/\lambda = \Delta t/T$. We see from Fig. 9 that maximum sharpness without extraneous polar loops is achieved when B/λ is as large as possible without admitting the first large secondary loop.

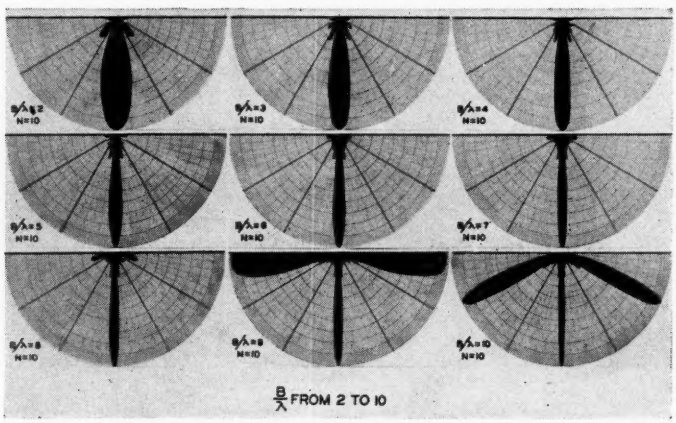

FIG. 9.

This may be accomplished by setting $\Delta t/T$ equal to the last root of equation (5) before the first secondary maximum, setting $\psi = 90°$, and solving for B/λ.

From (5) and Fig. 3 we see that the proper value of $\Delta t/T$ is

$$\Delta t/T = (N - 1)^2/N. \tag{13}$$

Putting this value for $\Delta t/T$ into (11) and setting $\psi = 90°$ we have

$$B/\lambda = (N - 1)^2/N \tag{14}$$

as the condition to be satisfied for maximum sharpness attainable without extraneous loops when the primary loop of the polar sensitivity curve points vertically downward.

The family of polars for which $B/\lambda = (N-1)^2/N$ is shown in Fig. 10.

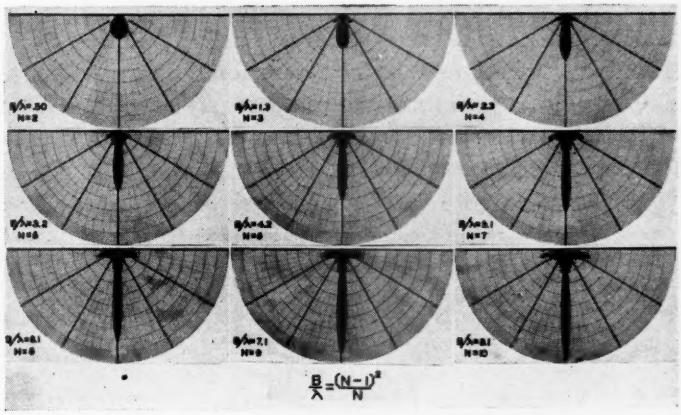

FIG. 10.

If, as frequently happens, the geophone interval is fixed, and a choice of the number of adjacent geophone outputs to be added is subsequently made, we have the relation

$$B/\lambda = K(N - 1)$$

where K is the geophone interval divided by the wave length.

In Fig. 11 the family of polars is shown for which $K=0.9$ or $B/\lambda = 0.9\ (N-1)$. For this value of K, part of the large secondary loops

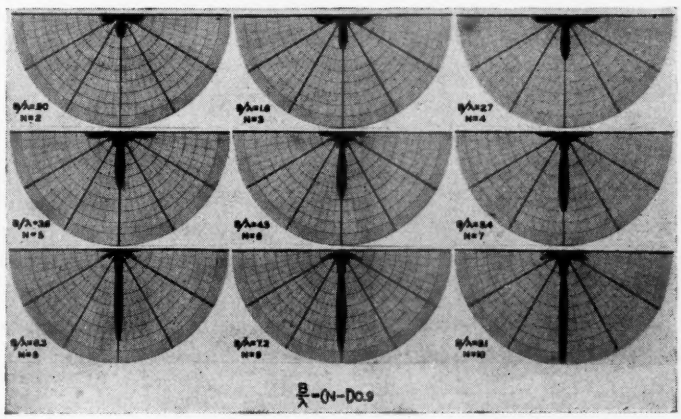

FIG. 11.

appear for $N=2$, decreasing slowly in amount until, when $N=10$, the polar is identical with that for $N=10$ in Fig. 10.

Thus, for $N>6$, the family of polars for the convenient case in which $B/\lambda=0.9\,(N-1)$ approximates the family for $B/\lambda=(N-1)^2/N$ where the primary loop has a maximum sharpness consistent with the exclusion of extraneous loops.

POLAR SENSITIVITY CURVES WITH CONTROL OF PHASE ANGLE OF CUMULATION

When outputs of the several geophones are recorded on adjacent reproducible sound tracks, as is done in the Sonograph Analyzer, time differences may be conveniently introduced between reproducing points on adjacent tracks. Referring to Fig. 1-B, this would be equivalent to taking a graphical summation at the ordinates erected at the points $1''$ to $5''$.

Equation (5), rewritten in terms of $\Delta t/T$ becomes:

$$A = \frac{\sin\left[\dfrac{N}{N-1}\pi\dfrac{\Delta t}{T}\right]}{\sin\left[\dfrac{1}{N-1}\pi\dfrac{\Delta t}{T}\right]}. \tag{15}$$

In Fig. 1-B we see that

$$\begin{aligned} \Delta t &= 2(1\cdots 1') = 2(1\cdots 1'') + 2(1''\cdots 1') \\ \Delta t &= \Delta t_0 + \Delta t'' \end{aligned} \tag{16}$$

where Δt_0 is the Δt setting of the analyzer apertures, and $\Delta t''$ is the Δt of the wave with respect to the line $1''$–$5''$ where cumulation takes place.

In equation (15), and Figs. 3 and 4, the time difference at which the waves were added was zero and Δt was measured with respect to zero. If the waves are added with a time difference other than zero, say Δt_0, equation (15) will still hold if the Δt therein is measured with respect to the time difference, Δt_0, at which the waves were added. Thus (15) holds for the case of rotated analyzer apertures if we replace Δt in (15) with $\Delta t''$ which is measured with respect to the setting at which cumulation occurs. Therefore, putting the value of $\Delta t''$ from (16) into (15) we have

$$A = \frac{\sin\left[\dfrac{N}{N-1}\pi\dfrac{\Delta t - \Delta t_0}{T}\right]}{\sin\left[\dfrac{1}{N-1}\pi\dfrac{\Delta t - \Delta t_0}{T}\right]}. \tag{17}$$

We may define $\psi_{\max}$ as the angle of arrival which will have a stepout of Δt_0 and hence yield a maximum sum.

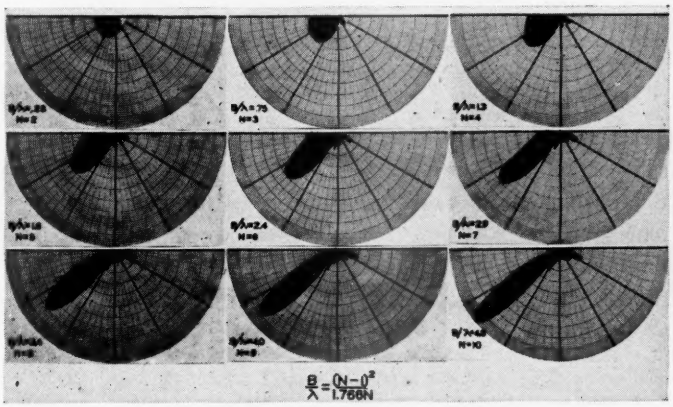

FIG. 12.

Then from (11)

$$\sin \psi_{\max} = (\lambda/B)(\Delta t_0/T) \tag{17a}$$

or

$$\Delta t_0/T = (B/\lambda) \sin \psi_{\max};$$

similarly

$$\Delta t/T = (B/\lambda) \sin \psi.$$

Putting these values in (17) we obtain

$$A = \frac{\sin\left[\dfrac{N}{N-1}\pi\dfrac{B}{\lambda}(\sin\psi - \sin\psi_{\max})\right]}{\sin\left[\dfrac{1}{N-1}\pi\dfrac{B}{\lambda}(\sin\psi - \sin\psi_{\max})\right]}. \tag{18}$$

In Fig. 12, $\psi_{\max}$ has been given the value of $-50°$. It is clear that if we had imposed the condition of Fig. 10

$$B/\lambda = \frac{(N-1)^2}{N}$$

and rotated the primary polar loop even slightly to the left, the large secondary loop would have appeared at $\psi = 90°$ at the right.

We may derive the equation to be satisfied by B/λ in order to maintain maximum sharpness while excluding unwanted secondary response loops for any direction, ψ_{max}, of the primary polar loop. When the analyzer apertures are set at Δt_0 we have from (11) and (16)

$$\sin \psi = (\lambda/B)(\Delta t_0 + \Delta t'') . \tag{19}$$

Equation (13) satisfies the condition for maximum sharpness while excluding secondary loops.

Since in equation (13) Δt was defined as measured with respect to the Δt of cumulation (there equal to zero) we must substitute $\Delta t''$ in (13) when the cumulation takes place at Δt_0.

From (13), where $\Delta t''$ is substituted for Δt, and (19), and setting $\psi = 90°$ we obtain

$$B/\lambda = \frac{(N-1)^2}{N} + \frac{\Delta t_0}{T} \tag{20}$$

combining (20) and (17-a) we have

$$B/\lambda = \frac{(N-1)^2}{N(1 - \sin \psi_{max})} \tag{21}$$

as the condition to be fulfilled for maximum sharpness without admitting secondary response loops.

In Fig. 12, B/λ has been given the value $(N-1)^2/(1.766N)$, indicated by (21). The family of polars then represents the sharpest primary loops which can be pointed towards a $-50°$ angle of arrival without introducing undesired secondary loops.

By the above expedient we have excluded the large secondary polar loop from the right side of the polar diagram. In so doing we have set a maximum value for B/λ. For small values of N, a larger value of B/λ is required to allow the response to reach zero at, or before, $\psi = 90°$ on the left side of the polar diagram. Another advantage of a large number of geophones, besides those illustrated in Figs. 6 and 7, has thus been demonstrated.

If the line of Sonograph Analyzer apertures is rotated, Δt_0, and hence ψ_{max}, the angle in which the primary polar loop points, will vary. Equation (18) may again be applied with ψ_{max} variable. The family of polar curves as ψ_{max} varies from 0° to −80°, $N=10$, and $B/\lambda=4.6$, is shown in Fig. 13. Since B/λ was calculated to exclude secondary polar loops for $\psi_{max}=-50°$, the first secondary loop appears at the right of the polar diagrams for $\psi_{max}=-60°$, $-70°$, and $-80°$.

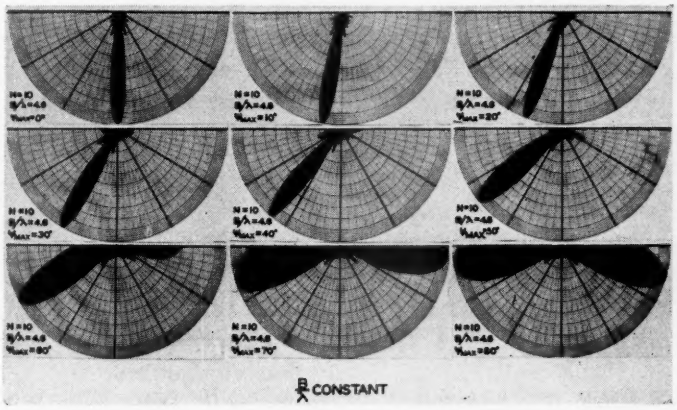

FIG. 13.

We could have chosen B/λ so that no secondary loops would have occurred for any value of ψ_{max}. Setting $\psi_{max}=-90°$ in equation (21) we see that for complete exculsion of secondary polar loops for any position of the primary polar loop,

$$B/\lambda = \frac{(N-1)^2}{2N} . \tag{22}$$

One will seldom find it necessary to fulfill the conditions of (22) or even to set $\psi_{max}=-50°$ in (21), for in practice the waves are usually modulated by exponential, or other transient waves,[9] and the secondary polar loops are considerably smaller than the primary. Furthermore, in specific areas the expectation of interfering waves in certain high-angle ranges may be negligible, and thus in these angular ranges considerable secondary response may be permissible.

Figs. 12 and 13 illustrate a control of the angular response curves readily attainable only with the Sonograph Analyzer. By this means it

is possible to obtain maximum response in any desired direction while substantially excluding waves arriving from other directions.

When geophones are direct-connected, the only way to obtain a large primary response to waves from moderately high angles in the plane of the geophones is to decrease the geophone spread far below 2λ, the value for which the upper left hand polar of Fig. 9 was plotted. By this method moderately high angle response is obtained only by a sacrifice in the sharpness of the primary polar loop—which must still point vertically downward.

In the Sonograph method, however, the reproducing apertures may be set to any desired over-all time difference, Δt_0, before cumulation, thereby obtaining a maximum response to the corresponding angle of arrival, ψ_{max}, while minimizing the response from other angles.

SUMMARY

(1) Many of the undesirable disturbances on reflection seismogram traces are due to a finite number of regular wave-fronts arriving at the geophones at the surface of the earth from different directions and existing in the seismogram with different stepouts or Δt's.

(2) Directional selectivity or "Δt selectivity" to eliminate many of these undesired waves may be obtained by connecting together several equally spaced geophones planted in a horizontal line at the surface of the earth.

All the following conclusions on this problem refer to steady state sinusoidal waves. They must be modified quantitatively but not qualitatively for other wave shapes.

(3) The response of such a group of direct-connected geophones to waves of known period arriving at the geophone group may be calculated as a function of the time difference of arrival at the extreme geophones in terms of the number of geophones connected. (Equation (5)), (Figs. 3 and 4).

(4) Maximum discrimination in favor of waves having zero Δt is obtained by connecting two spaced geophones together.

(5) The response of a group of direct-connected geophones to waves of known wave length and period arriving at the geophone group may be calculated as a function of the effective angle of arrival in the plane of the geophones in terms of the geophone spread and the number of geophones connected. (Equation (12)), (Figs. 8 to 11).

(6) Maximum discrimination in favor of waves arriving perpendicular to the line of geophones is obtained by connecting to-

gether as large a number, N, of geophones as convenient and making the geophone spread equal to $(N-1)^2/N$ times the effective wavelength.

(7) Substantial response to moderately high angles of arrival in the plane of the geophones may be achieved by making the geophone spread small. However, the direction of maximum response remains perpendicular to the line of geophones until the limiting case is reached where the geophone spread is zero and the response is equal for all directions.

(8) The individual geophone outputs may be separately recorded on adjacent reproducible sound tracks, as is done by the Sonograph recorder. In the process of reproduction with the Sonograph Analyzer, any desired time difference between adjacent sound tracks may be introduced before summing the waves.

(9) For the Sonograph method maximum discrimination in favor of waves arriving at any angle to the line of geophones is obtained by recording as many geophone outputs as convenient on adjacent reproducible sound tracks, introducing the appropriate over-all time difference between extreme sound tracks before adding (equations (17) and (18)) and making the geophone spread equal to $(N-1)^2/2N$ times the effective wave length (Figs. 12 and 13.).

(10) By the Sonograph method the direction of maximum response may be varied at will subsequent to recording, substantial reduction of the response to all other directions of arrival, *including the perpendicular to the line of geophones*, is obtained.

The author wishes to thank the members of the Rieber Laboratory Interpretation staff and especially Cyrus L. Clark, Sibyl M. Rock, and Reed Lawlor for valuable aid and criticisms made in the development of this work, and also wishes to thank William H. Gayman for reading the paper at the New Orleans meeting.

REFERENCES

1. Preston, T., *The Theory of Light* (London, 1895), p. 260.
2. Brown, G. H., "Directional Antennas," *Proc. I. R. E.*, Vol. 25, Jan. 1937, p. 78.
3. Born, W. T., "Notes on the Use of Multiple Shot Holes and Multiple Geophones," presented at the Dallas Convention, Soc. Pet. Geophysicists, Nov. 29, 1935.
4. Rieber, Frank, "Visual Presentation of Elastic Wave Patterns under Various Structural Conditions," GEOPHYSICS, Vol. 1., No. 2, July 1936.
5. Klipsch, P. W., "Some Aspects of Multiple Recording in Seismic Prospecting," GEOPHYSICS, Vol. 1, No. 3, Oct. 1936.
6. McDermott, E. E., "Use of Multiple Seismometers," *Petroleum Engineer*, Feb. 1937, p. 135.

7. Mott-Smith, M., "Adverse Effects with Variably Compounded Seismograph Records," GEOPHYSICS, Vol. 2, No. 3, July 1937 (and following discussion by Frank Rieber and C. H. Johnson).
8. Johnson, C. H., "Use of the Sonograph in Mapping Faults," GEOPHYSICS, Vol. III, No. 3, July 1938.
9. Hare D. G. C., "A New Source of Damped Wave Trains Suitable for the Testing of Geophysical Apparatus," GEOPHYSICS, Vol., 2, No. 4, October 1937.
10. U. S. Patent No. 2,051,153, and other patents pending.

THE FREQUENCY RESPONSE OF ELECTRO-MAGNETICALLY DAMPED DYNAMIC AND RELUCTANCE TYPE SEISMOMETERS*

DANIEL SILVERMAN†

ABSTRACT

The steady state shaking table has been used to determine the response, as a function of frequency and terminating resistance, of a dynamic and a reluctance seismometer. The observed response of the dynamic seismometer is shown to be identical with that predicted by theory. The response curves for the reluctance seismometer qualitatively substantiate analytical predictions as to the value of terminating resistance for maximum damping, and of the shift, with decreasing resistance, of the peak of response, to the higher frequencies. A short discussion of the electrical equivalent seismometer is given, and a comparison shown between the experimentally determined response of a reluctance type seismometer and that of its equivalent network.

INTRODUCTION

In seismic prospecting by the reflection method it is essential to have a detecting, amplifying and recording system that is capable of discriminating against the unwanted vibrations present in the ground at the time that the reflected wave reaches the surface. The ground roll generally determines the lower limit in frequency and the upper limit is set by wind vibrations and extraneous noises. Consequently, the working system must be frequency selective to a rather high degree, and it becomes necessary to have some means of determining the frequency response of the entire system. This is extremely important, for certain changes in discrimination may not only fail to accentuate the reflection, but may actually obliterate it and make the record more difficult to interpret.

Since the over-all response of the system is determined by each of the three parts, the detector or seismometer, amplifier, and recorder, it is essential to know the frequency response of each component. It has been, and is customary to determine the steady state response of the amplifier and recorder as a measure of the operation of the entire system. Heretofore it has been impossible to determine the exact response of the seismometer without very complicated equipment. However, by the use of the steady state shaking table as described by Kelly[1] the frequency response characteristic can be determined simply and rapidly.

* Paper read at Annual Meeting, New Orleans, La., March 15, 1938.

† Geophysical Laboratory, Stanolind Oil and Gas Company, Tulsa, Okla.

[1] Numbered superscripts refer to bibliography at end of the paper.

There may be some objection to the use of the steady state response as a guide in the choice of equipment because the ground vibration is composed of a number of transients in addition to more or less steady state components. Mathematical analysis shows that the response of a linear system to any type of transient force can be predicted once the response to a particular type of transient, namely the "unit function," is known. It is equally true that the response to any type of transient can be predicted if the entire steady state frequency characteristic is known. For practical purpose it is sufficient to know the response to steady state vibrations over and slightly beyond the working range of frequencies, namely the range of frequencies over which the output of the system is significant. Two different systems that show the same response over the working range will, for all practical purposes, show the same response to normal ground motion. In fact, the steady state frequency response is a more sensitive test of the similarity of two systems than is the field response since the type of impulse provided by the ground varies greatly from one territory to another. It has been observed experimentally that records taken in a given region by two seismometer-amplifier systems differing widely in their individual elements are almost indistinguishable provided the over-all steady state response of the two systems in the working region of frequencies are the same.

Many practical systems of seismometers and amplifiers utilize as one of their component elements a wave filter, which component is designed entirely on the basis of steady state measurements. Consequently, the steady state response characteristic is a very useful element in the design of recording equipment, and the shaking table provides the means of obtaining such a characteristic for the entire system, or for the seismometer alone.

RESPONSE OF THE DYNAMIC SEISMOMETER

The analysis of the response of the dynamic type of seismometer has been discussed in the literature, and has been shown to involve the solution of a differential equation of the form

$$\ddot{x} + C\dot{x}/M + Sx/M = m\ddot{y} \qquad (1)$$

where y is the amplitude of impressed displacement of the case,
x is the displacement of the mass relative to the case,
C is the coefficient of damping,
S is the spring constant,

M is the sprung mass, and
m is a constant.

This may be shown to follow from the summation of forces acting on the sprung mass of the seismometer due to an impressed vibration of the seismometer case.

Since the useful result of the seismometer is the voltage output, it is desirable to express the differential equation in terms of this voltage. The usual form of the equation is

$$\ddot{E} + C\dot{E}/M + SE/M = K\ddot{\dot{y}} = Kd^2(\dot{y})/dt^2 \qquad (2)$$

where E is the seismometer output voltage,
$\dot{y}$ is the amplitude of the impressed velocity, and
K is a constant of the system.

It is possible to express the output voltage in terms of the impressed displacement, velocity, or acceleration of the case. It is a matter of convenience that the velocity is used in this analysis, for it leads directly into the consideration of the equivalent seismometer, where velocity in the seismometer corresponds to voltage in the equivalent circuit.

Letting $S/M \equiv w_0^2$ and $C/M \equiv 2hw_0$, then (2) can be written as:

$$\ddot{E} + 2h\omega_0\dot{E} + \omega_0^2 E = Kd^2(\dot{y})/dt^2 \qquad (3)$$

where ω_0 is 2π times the natural frequency.

The significance of the factor h comes from the transient solution of equation (2), from which, for the case of critical damping, $C/M = 2\omega_0$. Thus h represents the percentage of critical damping, and is called the damping factor.

For steady state operation, the frequency of response of an oscillating system must be the same as the applied forced frequency. Therefore, in the steady state solution of equation (2) it is possible to assume that the response is of the same form as the impressed vibration, but differs by some phase angle, θ. Thus, for an impressed velocity of the form

$$y = y_0 \exp [j\omega t]$$

the response will be of the form

$$E = E_0 \exp [j(\omega t + \theta)].$$

Substituting in equation (2), and simplifying, provide the result:

$$\left| E_0/K\dot{y}_0 \right| = [(\omega_0^2/\omega^2 - 1)^2 + (2h\omega_0/\omega)^2]^{-1/2}. \tag{4}$$

Thus, for constant impressed sinusoidal velocity, the voltage output of the seismometer is given by

$$E_0 = K\dot{y}_0[(\omega_0^2/\omega^2 - 1)^2 + 4h^2\omega_0^2/\omega^2]^{-1/2}. \tag{5}$$

In general, there are three main points of interest about the response curves of a vibrating system, namely: the magnitude of the peak value, the relative sharpness of the peak, and the frequency at which the peak response occurs. For the case of zero damping which, of course, is never attained in practice, the peak value of voltage is infinite, and the frequency at which it occurs is called the resonant frequency of the system. As damping is applied to the system, the peak value is reduced, the shape of the curve changes, and the frequency at which the peak value occurs differs from the resonant frequency.

The change in frequency of peak response as a function of damping can be obtained from (4). It is sufficient to determine the value of ω for which the curve represented by (4) is horizontal, which occurs when E_0 is a maximum, or when the derivative of E with respect to ω is zero. Performing this differentiation, equating to zero, and simplifying, the relation between ω and h is found to be

$$\omega_0^2/\omega_M^2 = f_0^2/f_M^2 = 1 - 2h^2 \tag{6}$$

or

$$f_M = f_0/(1 - 2h^2)^{1/2}.$$

This indicates that as the damping is increased the frequency for the maximum response increases.

It is interesting to note that (6) shows the frequency for maximum response shifting to higher frequencies as the damping is increased. For many types of vibration problems the opposite trend is noticed, in which the frequency for peak response is lowered, when a constant impressed force is applied to the system and the damping increased.[2] This is explained by the differential equation, where in one case the amplitude of impressed *force* is held constant, and in the present case the amplitude of impressed *velocity* is held constant. For the case of constant impressed force the equation corresponding to (6) becomes

$$f_M = f_0(1 - 2h^2)^{1/2} \tag{7}$$

which shows that an increase in the damping factor, h causes a decrease in f_M.

A family of response curves for the dynamic seismometer is shown in Fig. 1, in which a comparison is made between the experimentally determined curves, and the mathematical response as predicted by (5). The curves shown are for various values of damping resistance, with the experimentally determined points indicated by crosses. The computed points are indicated by circles, and are plotted superim-

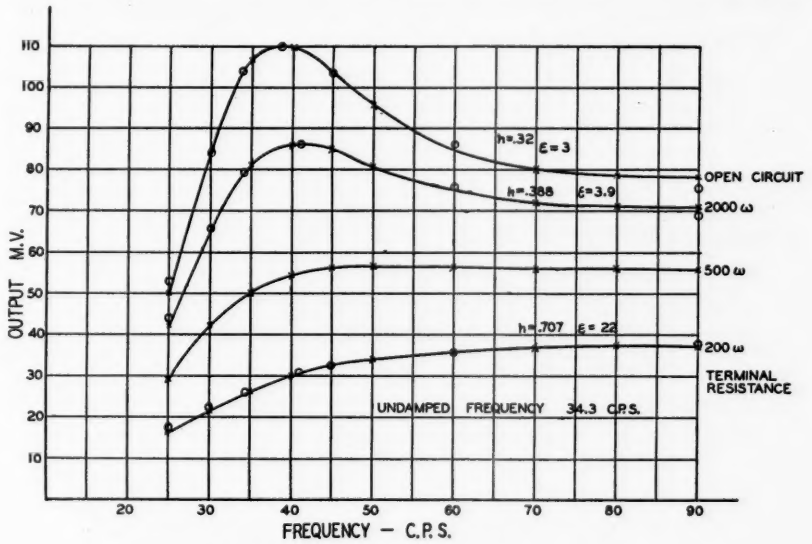

FIG. 1. Comparison of computed and measured steady state response curves for the dynamic type seismometer.

posed on the measured response curves, indicating an almost perfect check in the shape of the curve, in peak value, and in the value of frequency for peak response.

In computing the response of the dynamic seismometer it is necessary to know the resonant frequency, or angular velocity, ω_0, and the percentage of critical damping, h. Starting with the value of h and ω_0, a single value of response at any frequency serves to determine the constant, K, of the system from which the response of the system for any value of h can be determined. In the seismometer under consideration the coil was wound on an aluminum bobbin and it was impossible to remove all damping so that the value of ω_0 could not be directly determined. It was necessary to choose by trial and error,

values of ω_0 and h which would fit the curve corresponding to the open circuit case. Thereafter, using the value of ω_0 and the values of h computed from the drop in peak response, the other curves were computed.

RESPONSE OF THE RELUCTANCE SEISMOMETER

The computation of the frequency response of the balanced armature reluctance type seismometer for electromagnetic damping is quite laborious since it is determined by a third order equation of the form given by Washburn.[3]

$$\dddot{E}+R\ddot{E}/L+\omega_0^2[1+S''(L-L'')/(S-S'')L]\dot{E}+R\omega_0^2E/L = Kd^2(\dot{y})/dt^2 \tag{8}$$

where

$K = N\phi_g/Ll_g \times 10^8$
$\omega_0^2 = (S-S'')/M$
R = the seismometer coil resistance plus terminating resistance
L = the total inductance of the seismometer winding
L'' = the leakage inductance of the siesmometer winding
S = the spring constant
S'' = the equivalent spring constant of the magnetic pull
M = the mass of the moving system
N = the total turns in the siesmometer winding
ϕ_g = the average flux per gap
l_g = the effective length of air gap
E = the output voltage of the seismometer
$\dot{y}$ = the amplitude of impressed velocity.

Again assuming an impressed velocity of the form

$$\dot{y} = \dot{y}_0 \exp [j\omega t]$$

and a response of the same form

$$E = E_0 \exp [j(\omega t + \theta)]$$

and performing the indicated operations, the response is given by

$$|E/K\dot{y}_0| = [R^2(\omega_0^2/\omega^2 - 1)^2/L^2 + \omega^2\{(\omega_0^2/\omega^2 - 1) + \omega_0^2S''(L - L'')/(S - S'')\omega^2L\}]^{-1/2}. \tag{9}$$

As in the case of the dynamic seismometer, the shift of the frequency for maximum response can be found by differentiating (9) and equat-

ing to zero. This indicates the response curve has a zero slope at a value of ω/ω_0 determined by the equation

$$R^2/L^2 = (\omega_M^2/2\omega_0^2)\left[(\omega_0^4\{1 + S''(L - L'')/(S - S'')L\}^2 - \omega_M^4)/(\omega_M^2 - \omega_0^2)\right]. \tag{10}$$

It is difficult to get an explicit expression for ω_M in terms of R, but the following conclusions may be derived from (10):

1. For the case of $\omega_M = \omega_0$ the value of R is infinite. This is the case of zero damping.
2. For the case of ω_M less than ω_0 the denominator becomes negative and R/L is imaginary. This is an impossible condition, and therefore ω_M must be equal or greater than ω_0.
3. Again, for ω_M greater than,

$$\omega_0[1 + S''(L - L'')/(S - S'')L]^{1/2}$$

the numerator becomes negative and R/L is again imaginary. Therefore

4. ω_M is limited to ω_0 as a minimum value and

$$\omega_0[1 + S''(L - L'')/(S - S'')L]^{1/2}$$

as a maximum value. For ω_M between these two limits, R/L is real and positive.

The upper limit is not a fixed quantity but depends very definitely on the seismometer constants. The value of $(L-L'')/L$ is usually very near unity. But the value of $S''/(S-S'')$ may vary through wide limits. The nearer S'' approaches S the larger is this quotient, and the greater the range of shift in frequency.

In Fig. 2 is indicated a typical family of response curves for a reluctance type seismometer, as determined by shaking table measurements. As in the case of the dynamic seismometer the change in terminal resistance causes three important changes: in peak value, shape, and frequency of peak value. In both cases a decrease in resistance causes a lowering of the peak value and a shift to higher frequency of the peak response. The shape of the curve, or the relative width of the peak, which is an indication of the degree of damping, does not respond in the same manner to a lowering resistance. For the dynamic seismometer the damping increases monotonically with decrease in resistance. For the reluctance seismometer the damping first increases with decrease in resistance, reaches a maximum value, and then decreases with further drop in resistance.

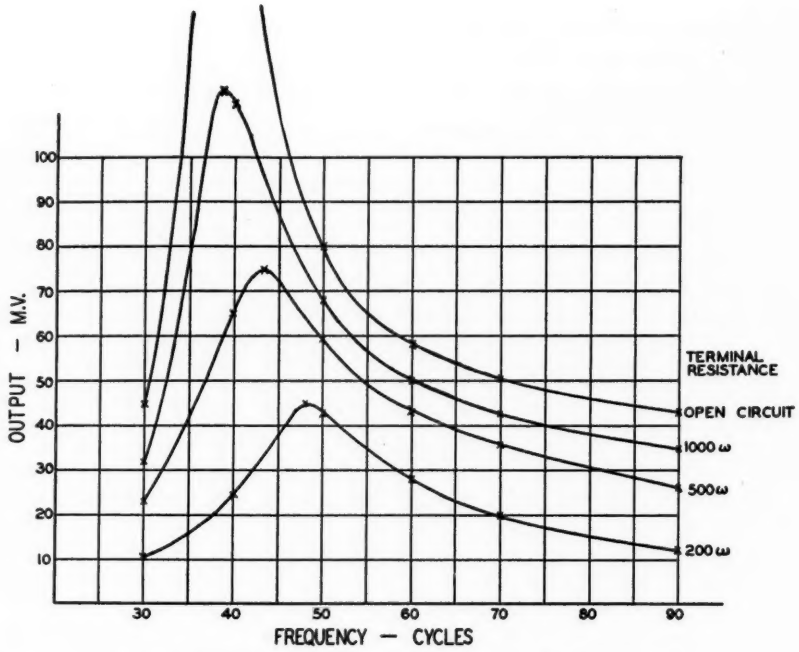

FIG. 2. Response curves of the reluctance type seismometer as measured on the steady state shaking table.

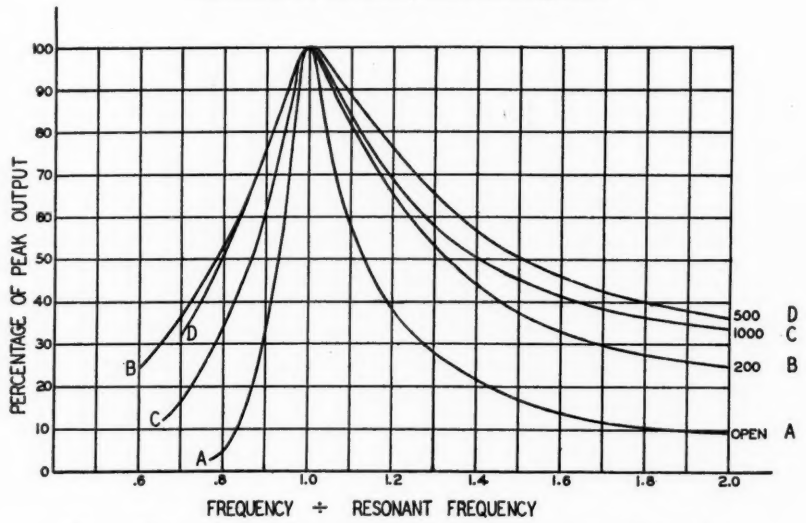

FIG. 3. Normalized response curves of the reluctance type seismometer for various values of terminating resistance.

This effect is due to the series inductance of the winding. For values of R large compared to the seismometer inductance the current is practically in phase with the voltage and damping is similar to that in the dynamic seismometer. As the resistance is decreased the damping current lags the generated voltage more and more, until the point is reached where further decrease in resistance, though increasing the current, actually causes a decreased component in-phase with the voltage, and the damping decreases.

The response curves of Fig. 2 for the electro-magnetically damped reluctance seismometer are replotted in Fig. 3 to normalized coordinates of frequency and amplitude. These serve to show more clearly the effect of damping resistance on the width of the resonance peak. As the terminating resistance is reduced from a very high value (open circuit) to values of 1000 ohms and 500 ohms the width of the curve increases, but as the terminal resistance is reduced still further to 200 ohms the curve becomes more peaked. Thus, on the premise that the damping is greater the wider the resonance peak, the value of terminal resistance of approximately 500 ohms provides the maximum value of damping for this seismometer.

DAMPING OF RELUCTANCE SEISMOMETERS

In the case of the dynamic seismometer the damping is easily expressed in terms of the damping factor, h, or the damping ratio, ϵ. By definition h is the percentage of critical damping, and ϵ represents the ratio of peak amplitudes of successive half cycles for the case of free damped oscillation. Both of these terms apply strictly to systems whose response is governed by a differential equation of the second order. For the electro-magnetically damped reluctance seismometer, for which the differential equation is of the third order, a new definition of damping must be agreed upon.

The value of ϵ for the dynamic seismometer can be determined by direct measurement on an oscillogram of the response to a unit function, which is very closely approximated by suddenly lifting a weight from the sprung mass. The response so recorded is a simple damped sinusoid. Under the same impulse the response[4] of the reluctance seismometer is the sum of an exponential and a damped sinusoid, and the ratio of the successive amplitudes of the sinusoidal component means less because the amplitude of the exponential term is not known.

It is convenient to define the damping of an electro-magnetically

damped reluctance seismometer in terms of its frequency response curve. Thus, if the response curve of the reluctance seismometer, when normalized with respect to peak frequency and peak amplitude, coincides with that of an ideal dynamic seismometer for which h and ϵ are known, it seems reasonable to apply these values of h and ϵ to the reluctance seismometer. Of course, an exact coincidence of the two curves will never be obtained for they are fundamentally of different shape. This is particularly true in the matter of the high

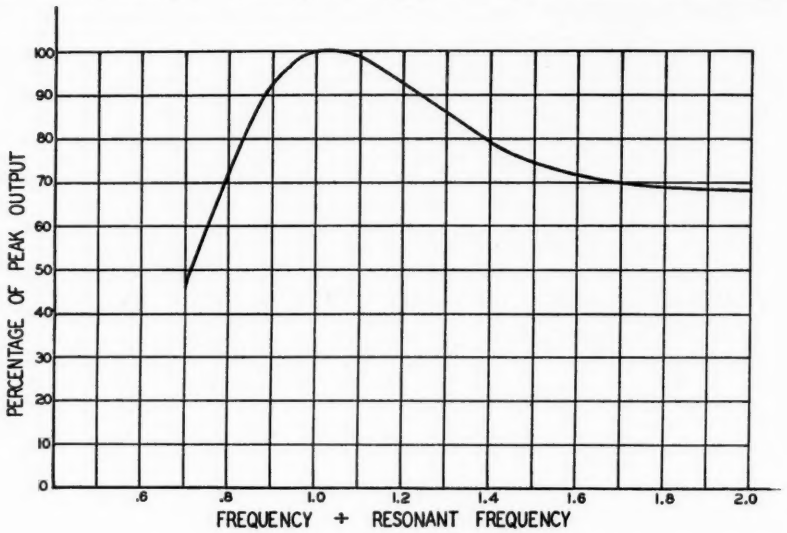

FIG. 4. Normalized response curve of a reluctance type seismometer adjusted for maximum damping.

frequency response. The response of a dynamic seismometer asymptotically approaches a constant value as frequency is increased (for constant amplitude of impressed velocity) while the reluctance seismometer, because of the cut-off effect of the series inductance and damping resistor, approaches zero output as the frequency becomes infinite. However, it has been found possible to obtain reasonable agreement between the response curves of dynamic and reluctance seismometers in the region of resonance, or from about 0.5 to 1.5 times resonance frequency.

The question may be asked as to what maximum value of damping is obtainable with a reluctance type seismometer. The lower the seismometer frequency the better the damping obtainable. Also, the

closer the negative spring content, S'', of the magnet pull approaches the spring constant, S, the better the damping, and in general, the less stringent the requirements for stability, the better the damping. Consequently the actual damping obtainable is very much a matter of the particular specifications of the seismometer. An electro-magnetically damped reluctance type seismometer has been built, which, with satisfactory field adjustment, has shown the response pictured in Fig. 4. On the basis of the above definition this corresponds to a value of h of about .35.

EQUIVALENT CIRCUIT OF THE RELUCTANCE SEISMOMETER

It has been shown[3] that the equivalent circuit of the reluctance type seismometer is of the form pictured in Fig. 5. This circuit has a differential equation identical in form to (8). The identity of the two differential equations indicates that measurements made of the response of the circuit should agree with that of the seismometer. On the basis of field tests of response to normal ground motion, and laboratory tests of the response of the circuit to voltages derived from

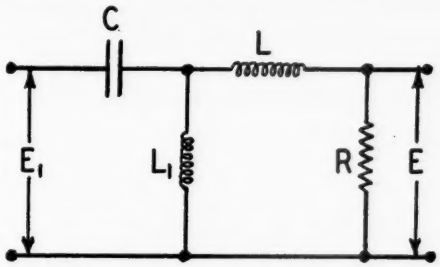

FIG. 5. Equivalent circuit of an ideal reluctance type seismometer.

normal ground motions, as described by Washburn, a satisfactory agreement was provided. However, similar experimental data obtained in different territories failed to entirely confirm this identity of response.

With the development of the steady state shaking table it became possible to compare the steady state response of the seismometer with the steady state response of its equivalent circuit. This comparison failed to provide a satisfactory agreement, which indicated that the two systems were not identical. Thus the differential equation (8) and the equivalent circuit of Fig. 5 must refer to an ideal seismometer, and not to the actual seismometer which was tested.

The real seismometer may differ from the ideal in a number of ways, particularly in the presence of a number of small losses which

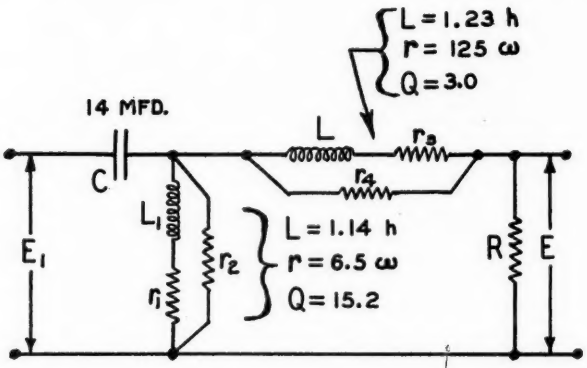

FIG. 6. Equivalent circuit of a real reluctance type seismometer.

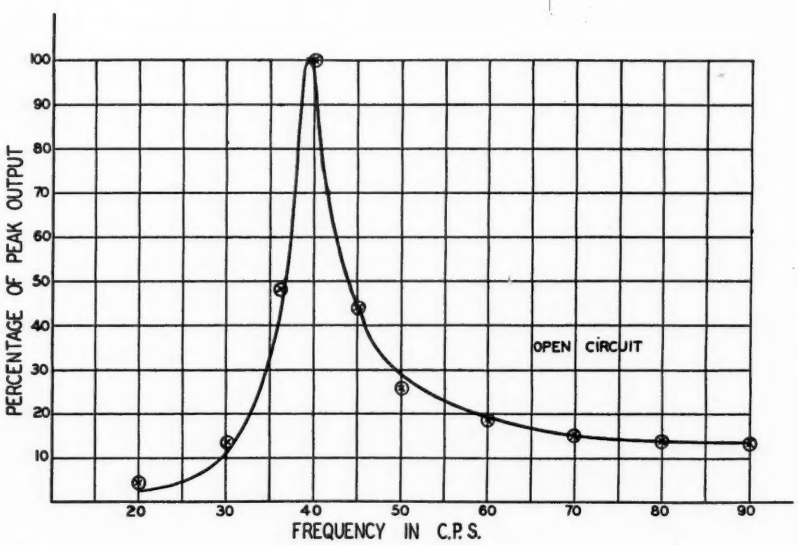

FIG. 7. Comparison of the steady state response of a reluctance type seismometer and its equivalent circuit for infinite damping resistance.

are known to be present, such as spring hysteresis, magnetic hysteresis and eddy currents, and air friction. In other words, in order to make the two systems really equivalent the "Q" of the corresponding

elements of the two systems must be the same. The Q of the two inductances of the circuit must be matched to those of the seismometer. The complete circuit of the equivalent seismometer might be represented to greater accuracy by Fig. 6, where the values of r_1, r_2, r_3, and r_4 are used in conjunction with ideal coils to provide the desired Q.

The computation of the response of a circuit of this form is quite laborious, and it becomes convenient to make use of the circuit itself

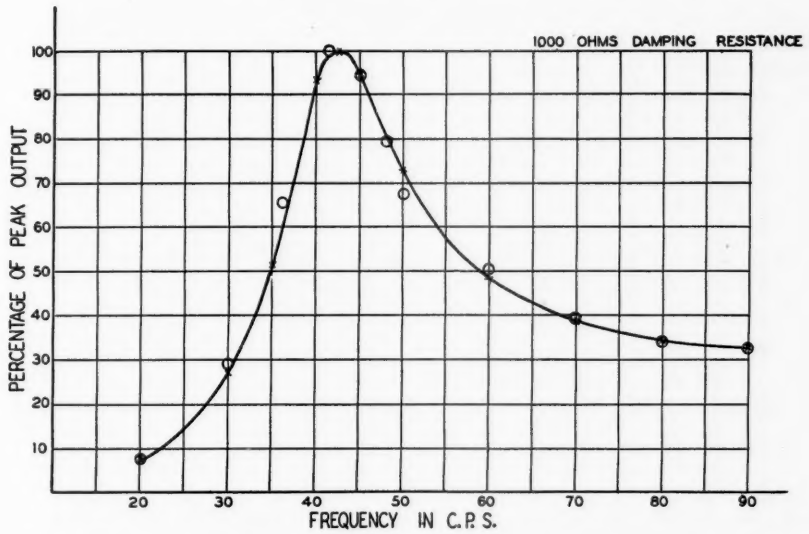

FIG. 8. Comparison of the steady state response of a reluctance type seismometer and its equivalent circuit for 1000 ohms damping resistance.

as a mathematical instrument. To do this an electrical circuit was set up in the laboratory, with its circuit elements determined partly by measurement of the constants of the actual reluctance seismometer, and partly by trial. The Q of the shunt inductance was determined by trial to check the response of the seismometer for the open circuit condition. Then the Q of the series inductance was determined by measurement of the winding of the seismometer. The constants of the actual coils are indicated in Fig. 6.

Comparisons are made in Figs. 7, 8, 9, and 10 between the observed response of the circuit, and that of the seismometer, for several values of terminating resistance. They show good agreement, indicat-

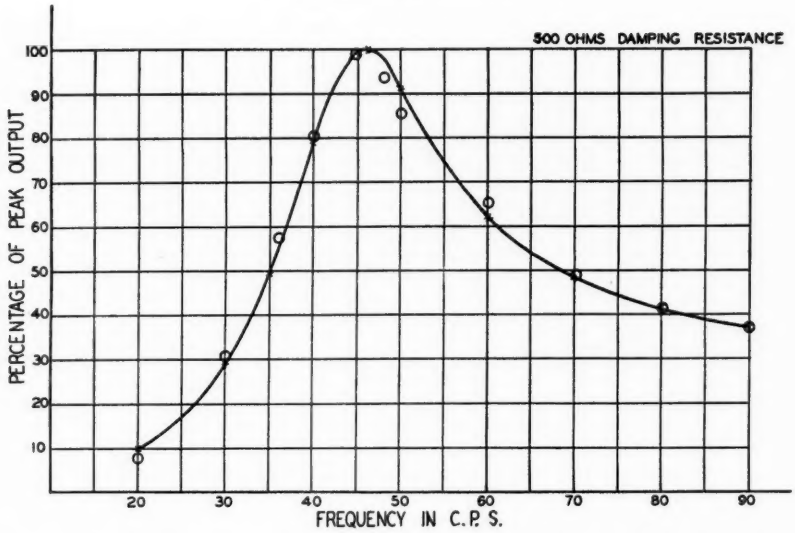

FIG. 9. Comparison of the steady state response of a reluctance type seismometer and its equivalent circuit for 500 ohms damping resistance.

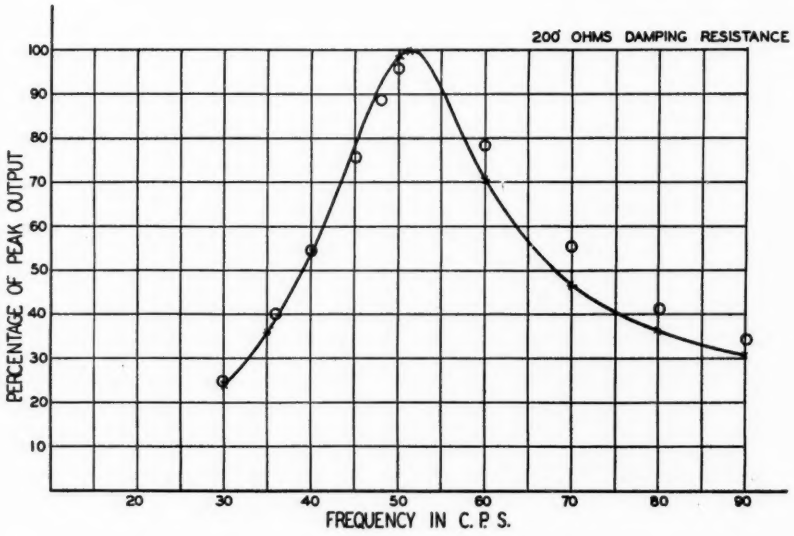

FIG. 10. Comparison of the steady state response of a reluctance type seismometer and its equivalent circuit for 200 ohms damping resistance.

ing that the circuit of Fig. 6 is really equivalent to the seismometer. In these curves, the experimental points for the seismometer are indicated by crosses, and the measured points for the circuit are indicated by circles. The slight variation indicated by the curve for 200 ohms is explained in part by the fact that the inductance values of the coils varied somewhat with current. Although carried only to slightly above 90 cycles, extrapolation of the response curves indicates good agreement far beyond this point. Since all the constants of the equivalent circuit are not derived from direct measurement on the actual seismometer, this circuit may not properly be called an equivalent seismometer, although once determined it can be used as one.

With the development of the steady state shaking table, however, the need of an equivalent seismometer for steady state measurements has been lessened. This is particularly true since it has been found that the equivalent seismometer must be more than just equivalent to the ideal seismometer. For each seismometer there is only one equivalent, and vice versa. And, in general, it is easier to make an equivalent circuit to represent a given seismometer than it is to build a reluctance seismometer to fit the constants of a given circuit. For transient measurements the equivalent circuit still has a wide field of usefulness. For steady state measurements the shaking table can be used very conveniently to obtain the separate seismometer response, or the over-all response of the system of seismometer, amplifier, and recorder.

CONCLUSIONS

In conclusion it may be said that the steady state shaking table is of extreme usefulness in the determination of the steady state response of an actual seismometer, either by itself, or in combination with other apparatus. The response so obtained is checked very closely by mathematical computation from the differential equation. The results of the use of the shaking table confirm the conclusions reached analytically concerning the value of resistance for maximum damping with the reluctance type seismometer, and the shift of the frequency of peak response with change in the value of damping. Lastly, the shaking table has provided a test of the equivalence of an "equivalent seismometer," and demonstrated its usefulness in the design and test of individual or complete electro-mechanical systems, such as the seismometer-amplifier-recorder systems used in seismic prospecting.

REFERENCES

1. Kelly, D., "Reaction Type Steady State Shaking Table." GEOPHYSICS, this number.
2. Timoshenko, S., *Vibration Problems in Engineering*. Van Nostrand, 1937. Page 41.
3. Washburn, H. W., "Experimental Determination of the Transient Characteristics of Seismograph Apparatus. GEOPHYSICS, Vol. II, No. 3, July, 1937. Page 243.
4. Sparks, N. and Hawley, P. F., "Maximum Electromagnetic Damping of the Reluctance Seismometer." GEOPHYSICS, this number.

A REACTION TYPE SHAKING TABLE*

DUNFORD KELLY†

ABSTRACT

A steady state shaking table utilizing the principle of reaction has been constructed for the measurement of the response of seismometers and the over-all response of seismograph apparatus. A mass of 500 pounds is driven at amplitudes of the order of 10^{-4} inches by a small eccentric mass which is rotated at the center of percussion of a bar, the upper end of which is pivoted to the bottom of the heavy mass. The amplitude of motion of the table top is independent of frequency between 10 cycles per second and an undetermined upper limit higher than 150 cycles per second.

REQUIREMENTS

Systematic development of seismograph apparatus (seismometers, filters, amplifiers, and recorders) requires that measurements be made of the response of each component of the system, and of that of the over-all system as it is to be used in the field. Measurements on the filters, amplifiers, and recorders can be made simply enough with the aid of an electric signal generator, constant impedance attenuator, and vacuum tube voltmeter. Measurements of the response of seismometers, and of any proposed complete system, require the aid of a shaking table, i.e., a mechanical signal generator.

A mechanical signal generator, like an electrical signal generator, should:

1) Have a constant output (of displacement, velocity, or acceleration) over the working range of frequency.
2) Be unaffected by the apparatus which it drives.
3) Have a signal level control.
4) Have a continuously variable control of the frequency of the signal.
5) Produce a signal in which the harmonic distortion of waveform is negligible.

The shaking table to be described meets not only these requirements but also the important requirement of low construction cost.

BASIC DESIGN

The general construction of the table can be seen in Fig. 1, and the construction of the shaker in Fig. 2. A large mass is suspended

* Paper read at Annual Meeting, New Orleans, La., March 16, 1938.

† Geophysical Laboratory, Stanolind Oil and Gas Company, Tulsa, Okla.

on springs so as to have a low natural frequency. To the bottom of this is attached a compound pendulum. The eccentric, which is the source of motion of the table, is motor driven through a short rubber coupling. The role of the pendulum is to prevent the horizontal thrust

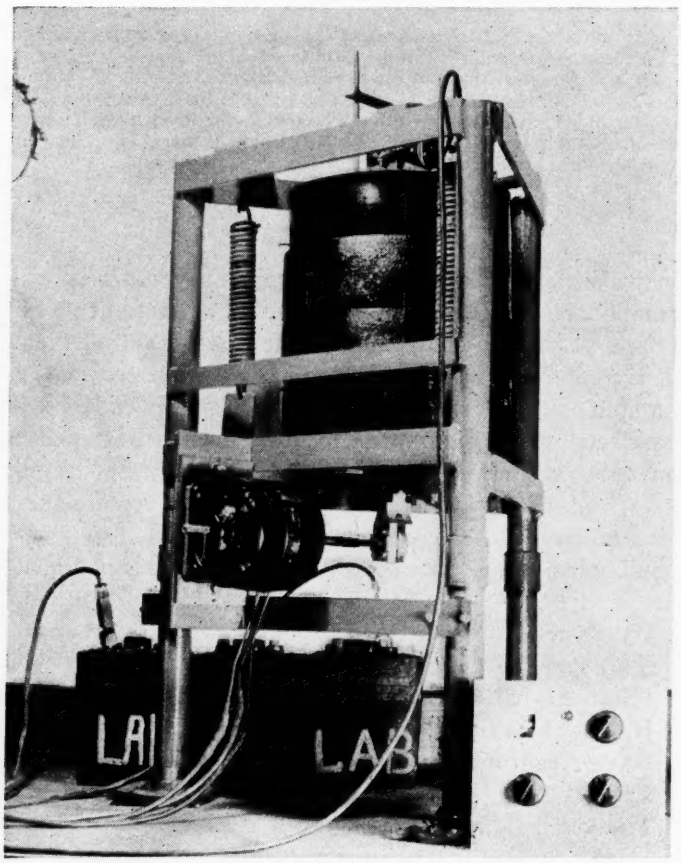

FIG. 1. Complete shaking table.

of the eccentric from rocking the large mass. (It is obviously desirable that the table have purely vertical motion.) It does this by virtue of the fact that a pendulum may be struck a horizontal blow at a certain point without transmitting any horizontal force through its axis. This point is the center of percussion. It is here that the axis of the eccentric is mounted.

Assuming for the moment that the large mass and spring system has so low a natural frequency that throughout the seismic range it acts as though the large mass were in free space, we can easily see what the nature of the motion of the large mass will be. As the only force which the pendulum transmits is vertical, the vertical force produced by the eccentric is the only one which need be considered. Since the eccentric is driven at constant velocity by the motor, the

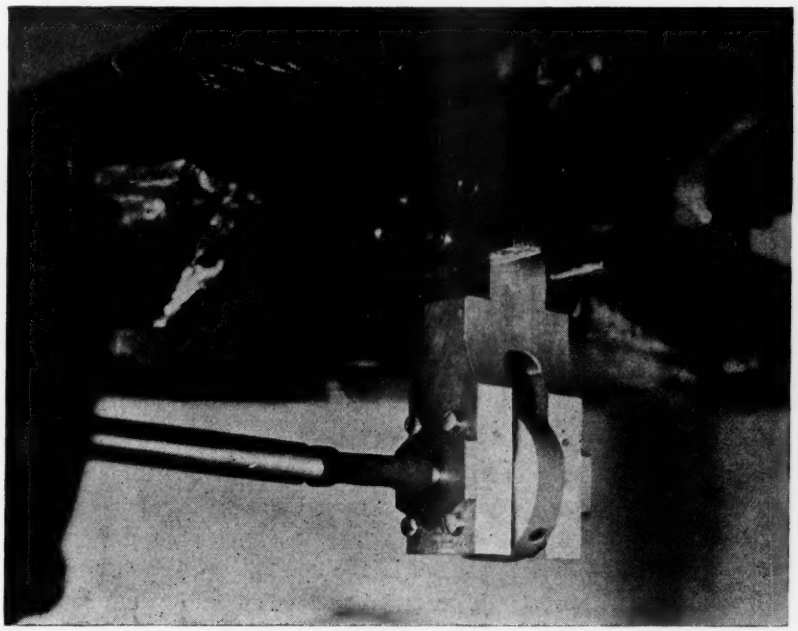

FIG. 2. Driving unit.

radial force produced by the eccentric is constant. The vertical component of this force is sinusoidal, since it varies as the cosine of the angle defined by the crank arm of the eccentric and this axis. Hence, the force on the large mass is

$$mr\omega^2 \cos \omega t = Ma$$

where m = eccentric mass
M = large mass
ω = angular velocity
t = time

r = radius (of eccentricity)
a = acceleration of large mass.

The acceleration of the large mass is sinusoidal and proportional to $mr\omega^2/M$, the velocity is sinusoidal and proportional to $mr\omega/M$, and the amplitude of the displacement is constant, and equal to mr/M.

The springs which support the large mass have some effect on its amplitude, but this effect can be kept negligible by making the natural frequency of the system low.

DESIGN DETAILS

The details of design of the shaking table may be of interest. The sprung mass of the table is 500 pounds, being made this heavy to prevent reaction on its motion from the device to be tested. The necessary mass of the table is determined by the mass and damping of the moving systems to be tested. For instance, assume that the moving mass of the largest device to be tested is 2 pounds and its damping allows its amplitude to be 5 times the driving amplitude at resonance. Under these conditions the force exerted by the 2 pound mass will be equivalent to that produced by 10 pounds having the same amplitude as the table; and in the case of the 500 pound table, the effect on its amplitude will be 2%, a reasonable figure. Another design factor is the natural frequency of the sprung mass. By making this very low relative to the frequencies to be measured, the restoring forces of the spring may be made negligible in comparison with the forces which accelerate the mass. A natural frequency of 2 cycles per second with damping provided by felt packed in the coil springs kept the amplitude constant within 2% down to 10 cycles. The next item for consideration is the length of the pendulum to be used in eliminating the horizontal forces. A natural frequency of about 3 cycles was found satisfactory. The mass and throw of the eccentric to be used are limited on one extreme by the amount of natural and artificial ground unrest which is transmitted to the shaking table through its supporting springs. This motion will indicate on the output meter along with the desired signal, so the forced motion of the table must be an order of magnitude greater. The other limit is the allowable load on the bearings and the amount of wave-form distortion which can be tolerated. The effect of large motions of the pendulum is comparable to that of a large crank throw on a short connecting rod. It produces harmonic distortion. Due to these limits on the practical range of amplitude, this table has a minimum amplitude of 5×10^{-6}

inches and a maximum amplitude of 10^{-3} inches. In order to be able to change the amplitude quickly, the eccentric, Fig. 3, is made in two parts, one eccentric within another, so they can be shifted, one relative to the other, thus changing the over-all eccentricity. The bearing connecting the pendulum to the large mass is a slotted bushing with a clearance adjustment. The bearings on which the eccentrics are mounted are preferably closely fitted plain bushings, but if the forces involved require them, super precision ball bearings may be

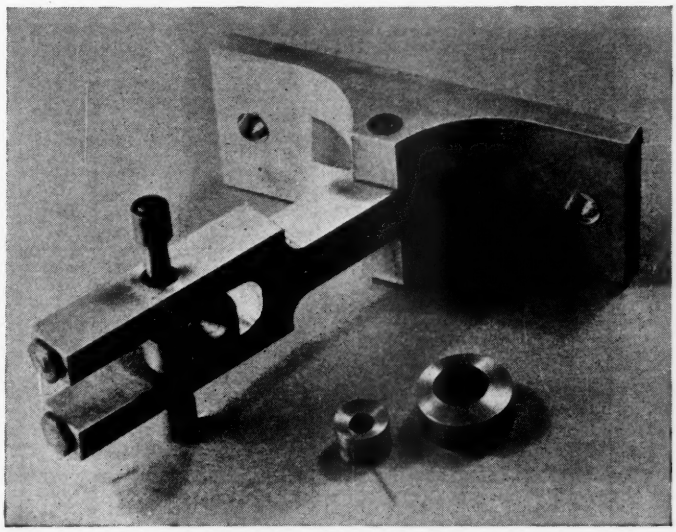

FIG. 3. Details of eccentrics.

used. The final unit in the machine is the power source for the eccentric. It is a shunt wound, battery operated electric motor coupled to the eccentric by a short length of rubber tubing. The motor has good speed regulation between 600 and 9000 R.P.M. or 10—150 cps. In using the shaking table some additional equipment is required. One necessity is a frequency meter. In this case an oscilloscope is used to produce Lissajous figures resulting from the rectangular combination of the output of a seismometer and voltage taken from the 60 cps lighting circuit. Another component is an amplifier having negligible amplitude and frequency distortion, which raises the output of the device under test to a sufficient level to be read on a vacuum tube voltmeter.

This table produces constant amplitude sinusoidal displacements. Although the response of a seismometer to this type of motion is of interest, we prefer to measure the response to constant amplitude of velocity, for several reasons: the differences between instruments are thereby emphasized; in the electro-mechanical analogue which we find convenient to use, E.M.F. is analogous to velocity. There are two methods of producing curves of the response to constant amplitude

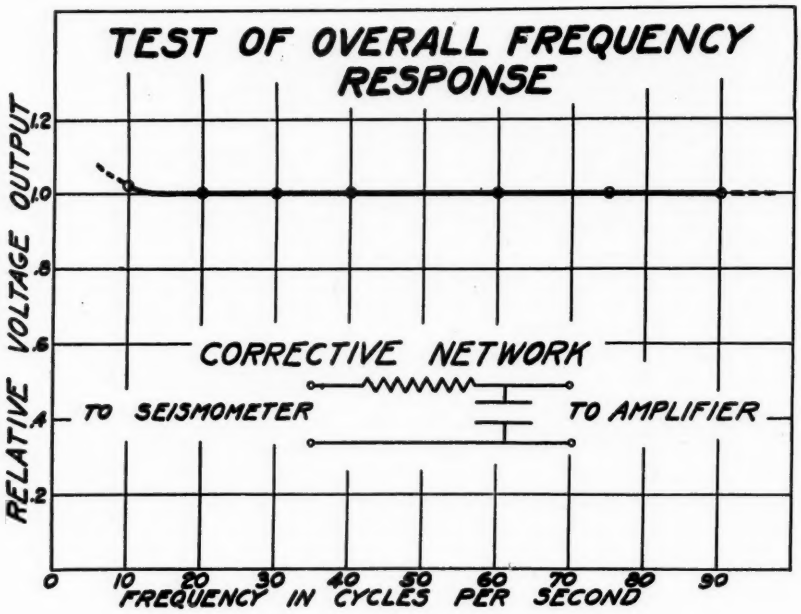

FIG. 4. Over-all frequency response.

of velocity. One is to divide all measured seismometer output voltages by their respective frequencies, and the other is to use an electrical network which accomplishes the same result. The latter method was chosen. The network which is used is very simple, comprising a resistor and condenser, Fig. 4, interposed between the seismometer and the amplifier. With the constants which were chosen, the device operated with negligible error. The validity of the use of either method, of course, rests on the correctness of the assumption that the seismometer behaves as a linear system. Experiment verified this, for the small motions being used.

MEASUREMENTS OF MOTION

When the shaking table was completed, numerous tests were made to insure proper operation. A check of the variation of amplitude with frequency was made with the aid of a very low frequency dynamic "seismometer," which consisted of a permanent magnet clamped to the top of the shaking table, and a coil which was suspended from the earth (by a spring giving a natural frequency of about one cycle). This coil fitted over the permanent magnet. It was connected to the electrical corrective network, through the flat amplifier, to the vacuum tube voltmeter. The variation of voltage with frequency was slight, as shown in Fig. 4. By using seismometers having only horizontal response, the amount of horizontal motion of the table was measured, and found to be never greater than five per cent of the vertical motion. Measurements of the bearing noise and harmonic content appearing in the output were also made, and showed practically no lower order harmonics, while the upper harmonics and bearing noise did not affect the voltage readings although they were visible in the oscilloscope.

PRACTICAL APPLICATION

Several months of use of this shaking table have shown that it gives reproducible results, requires no corrections for variations in output, and is nearly as rapid in use in the determination of the frequency response of the electromechanical systems used in seismic prospecting as an ordinary electrical signal generator is in the determination of the response of purely electrical networks.

REVIEW

Architecture of the Earth. Reginald Aldworth Daly. D. Appleton-Century Company, 1938, 200 pp. 152 illus. $3.00. (The Century Earth Science Series, Kirtley F. Mather, Editor.)

Daly's earth model has a solid crystalline crust varying in thickness but not exceeding fifty miles. This crust encloses a continuous layer of vitreous rock, relatively thin, which rests on a denser vitreous material. The heavier substratum surrounds a so-called "iron core" possibly crystallized by high pressures of the interior. This vitreous subcrust has some properties of a solid; hence, it behaves more or less like a rigid mass.

The world map may be used as a cloak for Daly's earth model. It will show many details essential to the constituents and physical properties of the earth crust, with possibly some hints pertaining to the subcrust.

Oceans and continents are the two major physical features comprising the earth's surface. The continents are like huge curved bucklers, "Continental Bucklers," rising about two and a half miles above the ocean bottom. Four distinct systems of rocks constitute the make-up of these "Bucklers," (1) a continuous assemblage of rocks called "Basement Complex," or "Baffling Complex," which is partially covered by (2) veneers of layered sediments, and (3) regional veneers of lavas derived from the basaltic crust and vitreous substratum below and erupted through fissures into the "Basement Complex," finally, (4) regional ice caps and glaciers. The ocean waters rest on basaltic rocks. Exceptions are the continental shelves, the Atlantic Swell, subsea areas of the Indian Ocean, the New Zealand region, and areas off the west coast of South America. These are similar in rock composition to that of the "Continental Bucklers." A basaltic crust, then, is postulated which extends completely around the earth.

Geophysics has aided greatly in approximating the constituent parts of Daly's earth model. Seismic data corroborate denser rocks for the ocean floors, namely basalts. Rocks of higher velocities, therefore heavier, are found underneath the lighter rocks of the continents. Further, Gutenberg's shadow zone becomes highly significant. It postulates a substratum somewhat lighter than the crystallized materials above, but, like the rocks above, increasing in density with depth.

The lighter vitreous subcrust immediately below the heavier crystalline crust probably accounts for crustal deformation. Mountain chains invariably have risen out of geosynclinal troughs. Their uplift occurred after intense folding and crumbling, resultant of compressive forces from the limbs of the geosynclines pulled toward each other by gravitational foundering of downdip segments of these geosynclines.

Exactly reversed to the forces of mountain building is the energy that produces regional lava flows and innumerable volcanoes within mountain ranges. The weight of the crust produces heat sufficient to melt all rocks. This rock melt becomes vitreous and homogeneous. Being ligher than the crystallized crust above, the liquids rise through cracks, vents, and fissures with explosive force.

Not all lava flows and volcanic materials are basalts. Great volumes of intermediary and acidic melts are intruded into and poured over mountain roots. Liquid basalts of the upper substratum encroach upon the slightly heavier crust above, melt, incorporate them, and invade the crystalline sedimentary roots. Huge blocks fall into the liquids. They melt. Chemical assimilation results. As the lighter constituents increase, densities of the melt change continually. Convection currents originate, pushing

the acidic melt to the top. These are intruded into surrounding rocks and frequently extruded as lava flows and volcanoes.

Would fragmentation of huge crustal blocks, their foundering, and simultaneous rising of thick tongues of lavas imply insecurity for the crust of this earth model? No catastrophic sinking of the crust will take place for at least another half billion years. Geological and geodetic data prove that the earth crust is comprised of heterogeneous segments. The "Continental Bucklers," although thicker, are lighter than the ocean segments. Finally, there is rather definite proof that these segments are at equilibrium with each other.

Daly took the earth, brought it down to man's size, dissected it, and put it together again. This process was executed lucidly and intelligibly.

A. P. WENDLER

RECENT PAPERS OF INTEREST TO EXPLORATION GEOPHYSICISTS

The following papers, appearing in the "Transactions of the American Geophysical Union, 1938," published by the National Research Council, are of general interest to the Exploration Geophysicist:

Investigation of the Vertical Gradient of Gravity. Sigmund Hammer.

Formulas and Tables for the Deflection of the Vertical. Walter D. Lambert.

Geologic Interpretation of Gravity-Anomalies in the Northeastern United States. Chester R. Longwell.

The Effect of Geologic Corrections on Gravity-Anomalies. George P. Wollard.

A Proposed Investigation of Vening-Meinesz Anomalies. Maurice Ewing and H. H. Pentz.

A Study of Certain Reductions and Adjustments in Pendulum Observations. Albert J. Hoskinson.

Geophysical Investigations of the Geologic Structure of the Coastal Plain. George P. Wollard, Maurice Ewing, and Meredith Johnson.

An Electromagnetic Method of Determining Induction Coefficients of Magnetometer Magnets. J. H. Nelson.

Testing the Orientation of a Declination Variometer by its Temperature Coefficient. H. Herbert Howe.

Alternating Current Method of Measuring Magnetic Polarization of Rocks. E. A. Johnson.

Magnetization of Sediments from the Bottom of the Atlantic Ocean. A. G. McNish and E. A. Johnson.

Preliminary Report on Measurements of Magnetization of Oceanic Sediments. A. G. McNish and E. A. Johnson.

Application of Vertical Variometer Measurements to the Study of Secular Magnetic Variations. Victor Vacquier.

Notes on Horizontal Pendulum Observations in Relation to Certain Phenomena. F. Napier Denison.

Superposition in Interpretation of Resistivity Data. Irwin Roman.

Geomagnetic Investigations of the University of North Carolina. Wm. F. Prouty.

Magnetic Work of the United States Coast and Geodetic Survey, April 1937 to March 1938. E. W. Eickelberg.

Progress Report on Researches in Terrestrial Magnetism and Electricity at Department of Terrestrial Magnetism, Carnegie Institution of Washington, for year April 1937 to March 1938. J. A. Fleming.

THE SOCIETY ROUND TABLE

ANNOUNCEMENT OF ANNUAL MEETING

The annual meeting of the Society will be held in Oklahoma City, Oklahoma on March 21–23, 1939. Details and program will be announced later. Papers to be read should be sent to

Dr. F. M. Kannenstine
2011 Esperson Bldg.
Houston, Texas

MEMBERSHIP APPLICATIONS APPROVED FOR PUBLICATION

The executive committee have approved for publication the names of the following candidates for membership in the Society. This publication does not constitute an election, but places the names before the membership at large. If any member has information bearing on the qualifications of these nominees, he should send it to the Secretary within thirty days. (Names of sponsors are placed beneath the name of each nominee.)

ACTIVE

Robert Harrison Bliss, Jr.
Leo Horvitz, Robert Saibara, Alvin Jaques

Charles Lindsey Clark
Eugene McDermott, J. E. Jonsson, Barney Fisher

Dugger E. Cook
C. H. Dresbach, G. B. Lamb, E. A. Eckhardt

Craig Ferris
L. M. Mott-Smith, P. B. Brown, Stuart Sherar

Roy Lee Gallaway
C. C. Zimmerman, L. A. Scholl, Jr., Alexander Wolf

Albert Fred Haber
L. F. Athy, H. R. Prescott, E. V. McCollum

Robert Breck Moran, Jr.
Cecil E. Reel, W. A. English, Chester J. Donnally

Lowell Waller Saunders
Cecil E. Reel, Michael A. Boccalery, Chester J. Donnally

Charles A. Swartz
E. A. Eckhardt, Morris Muskat, B. Perkins, Jr.

Clifford Arthur Wachter
Herbert Hoover, Jr., H. Hart Pratley, H. Washburn

Richard Montague Walford, Jr.
A. E. Mix, J. C. Pollard, R. M. Wilson

Floyd James Williams
O. T. Lawhorn, J. E. Jonsson, Barney Fisher

Niles B. Winter
E. L. DeLoach, John A. Gillin, K. K. Spooner

ASSOCIATE

Cyrus Harold Acheson
F. G. Boucher, D. C. Barton, D. P. Carlton
Joe Cris Berger
R. G. Elms, O. T. Lawhorn, J. E. Jonsson
Donuil Marshall Hillis
Joshua L. Soske, Beno Gutenberg, Dean Walling
Danilo Ramaccioni
(Article III C-1 of the Constitution)
N. Allen Riley
J. C. Pollard, Henry C. Cortes, T. I. Harkins
Richard Boyden Rutledge
T. A. Manhart, A. J. Barthelmes, E. E. Rosaire
Jose Steider
J. W. Hoover, K. E. Burg, J. E. Jonsson
Russell Maurice Tripp
Roland F. Beers, W. W. Newton, Dart Wantland
Charles Edward Williams
John J. Rupnik, A. J. Hibbler, Louis A. Scholl, Jr.

TRANSFER FROM ASSOCIATE TO ACTIVE

John Doering

The ballot reprinted below was mailed all active members of the Society of Exploration Geophysicists on January 10, 1939. Active members who failed to receive ballots may secure them by notifying J. F. Gallie, Business Manager, P.O. Box 2181, Houston, Texas, that they failed to receive their copies. *Only active members who have paid 1939 dues are eligible to vote.*

OFFICIAL BALLOT

FOR THE YEAR MARCH, 1939—MARCH, 1940

For the Election of Officers for the

SOCIETY OF EXPLORATION GEOPHYSICISTS

FOR PRESIDENT AND VICE-PRESIDENT

Vote once for President (First Choice) and once for Vice-President

	FIRST CHOICE (FOR PRESIDENT)	SECOND CHOICE (FOR VICE-PRESIDENT)
W. T. BORN	☐	☐
H. C. CORTES	☐	☐
E. A. ECKHARDT	☐	☐
_____	☐	☐

FOR SECRETARY-TREASURER

VOTE ONCE

J. H. CROWELL	☐
E. R. MELTON	☐
_____	☐

FOR EDITOR

VOTE ONCE

ROLAND F. BEERS	☐
J. E. OWEN	☐
R. D. WYCKOFF	☐
_____	☐

After voting, place in accompanying official envelope, which should then be signed and mailed to the

SECRETARY-TREASURER,

H. B. Peacock
825 Esperson Bldg.
Houston, Texas